1967

A study of the growth of the inhibiting aluminum-roch alloy layer formed on steel during galavanizing in aluminum-bearing zinc

Angelo Richard Borzillo
Lehigh University

A STUDY OF THE GROWTH OF THE INHIBITING ALUMINUM-RICH ALLOY LAYER FORMED ON STEEL DURING GALVANIZING IN ALUMINUM-BEARING ZINC

by

Angelo Richard Borzillo

A Thesis

Submitted to the Graduate Faculty

of Lehigh University

in Candidacy for the Degree of

Master of Science

Lehigh University

1967

CERTIFICATE OF APPROVAL

This thesis is accepted and approved in partial fulfillment of the requirements for the degree of Master of Science in Metallurgy and Materials Science.

11 September 1967
(Date)

Walter C. Hahn, Jr.
(Professor in Charge)

W. F. Hosford
(Head of the Department)

ACKNOWLEDGMENTS

The author is indebted to many who made contributions towards this work. These include:

Professor W. C. Hahn, Jr. for his guidance and counsel,

Mr. L. E. Peters of the Bethlehem Steel Corporation for his resourceful assistance in preparing the test specimens and in determining the gravimetric data, and

Messrs. G. W. Ruyak, L. R. Salvage, T. L. Peters, H. L. Miller, F. H. Ruch and I. H. Fisher of the Bethlehem Steel Corporation for their metallographic, electron-probe, electron microscope, X-ray diffraction and chemical analyses.

Grateful acknowledgment is also due the Bethlehem Steel Corporation for the generous contribution in time, equipment and materials which made this work possible. Furthermore, special appreciation is acknowledged for the financial assistance of the Bethlehem Steel Corporation which covered tuition costs for the author's entire master's degree program.

TABLE OF CONTENTS

TABLE OF CONTENTS--CONT'D.

LIST OF FIGURES

LIST OF FIGURES--CONT'D.

LIST OF FIGURES--CONT'D.

LIST OF TABLES

LIST OF TABLES--CONT'D.

ABSTRACT

The growth of the aluminum-rich alloy layer was studied quantitatively by a chemical stripping method on galvanized coatings made in pure zinc baths containing about 0.2 and 0.3 per cent aluminum with varying contents of iron. The growth of this layer was found to be parabolic and a function of bath temperature and the aluminum/iron ratio of the bath. The thickness of the layer was estimated to range from about 0.1 to 0.8 micron.

Surface x-ray diffraction analysis showed that the layer is comprised essentially of Fe_2Al_5. However, positive identification of an iron-zinc-aluminum ternary phase was made by electron-probe micro-analysis, indicating that the layer has a duplex nature. Relation of these results to electron microscope examination indicated that the ternary transformation phase grows on the alloy layer surface as geometrically shaped nodules.

Based on these observations, a hypothesis was suggested for the growth of the alloy layer and subsequent breakdown of inhibition. Early stages of growth favor Fe_2Al_5 formation. Later, local transformation to the ternary phase occurs and both Fe_2Al_5 and the ternary phase may be growing simultaneously. Eventually, breakdown of inhibition occurs when the Fe_2Al_5 layer is consumed or penetrated during transformation to the ternary phase which then leads to growth of iron-zinc phases.

INTRODUCTION

Hot dip galvanized coatings are among the most extensively used metal coatings for the protection of steel. Basically, the two methods of application of galvanized coatings are the batch and continuous processes.

The batch process is used for coating small parts, such as fasteners and hardware, and large individual shapes, such as structurals and guard rail. These parts usually do not require fabrication after galvanizing; thus, good coating ductility and formability are not required on batch process coatings. Utilization of a flux to achieve galvanizing and relatively long immersion times (minutes) are common to all batch processes.

The continuous process is used to coat steel sheet, ranging from about 8 to 30 gage, continuously. Continuous processes are characterized by short immersion times, usually a few seconds, and utilization of gaseous surface preparation or aqueous fluxes to achieve galvanizing. Subsequent fabrication of continuous galvanized sheet into a wide variety of products requires the coating to be ductile and able to withstand severe deformation without flaking. Thus, the thickness of the brittle iron-zinc alloy layer which forms at the steel-zinc interface must be controlled and minimized to give good coating adherence and ductility. Control of the growth of this brittle alloy layer is achieved by adding about 0.10 to 0.25 per cent aluminum to the zinc bath.

Inhibition of the growth of the iron-zinc alloy layer by aluminum additions had been recognized for many years. However, only very small aluminum additions, usually less than 0.02 per cent, were added to the bath to improve the brightness of the coating. Additions necessary to control alloy layer growth, about 0.20 per cent, were not used because galvanizing was done mainly by the batch process which did not require highly ductile coatings. Moreover, such large aluminum additions reacted with the fluxes floating on the surface of the bath, causing coating difficulties. However, with the advent of the continuous process about 20 years ago, aluminum additions came into widespread use because of the necessity to produce a ductile, non-flaking coating.

Since that time, many investigators have studied the galvanizing reaction in aluminum-bearing zinc baths and have attempted to determine the mechanism by which aluminum inhibits iron-zinc alloy layer growth. Work reported in the literature indicates the presence of an aluminum-rich alloy layer at the steel-zinc interface in an aluminum-bearing galvanized coating. However, the mechanism by which this aluminum-rich alloy layer inhibits iron-zinc alloy layer growth is not clearly understood.

The purpose of this work was to determine the rate of growth of the inhibiting aluminum-rich alloy layer, to identify the compounds that comprise it and to examine the nature of its growth. Specifically, the weight of the aluminum-rich alloy layer was measured as a function of time and temperature on coatings made in Special High Grade zinc baths

containing 0.20 per cent and 0.30 per cent aluminum. In addition, low and intermediate iron levels were studied in the 0.20 per cent aluminum bath and only the low iron level was studied in the 0.30 per cent aluminum bath. Five immersion times were used for each bath composition at temperatures of 430°C, 450°C and 470°C. Growth characteristics of the layers and phases were studied with the optical and electron microscopes, the electron-probe microanalyzer, and X-ray diffractometer.

REVIEW OF LITERATURE

The following review does not cover all prior work on the effect of aluminum in galvanizing baths. Instead, a chronology of the development of the most pertinent findings, with experimental conditions, is discussed.

The most comprehensive single work covering the entire subject of hot dip galvanizing is that by Bablik.[1] In this book, he covers galvanizing theory as influenced by bath and steel composition, the fluxing reaction and practical operating aspects. In general, the data were obtained on still specimens mainly in iron saturated baths for relatively long immersion times. He noted that aluminum initially delayed the reaction between liquid zinc and solid iron for short immersion times; however, after initiation of the reaction, the iron attack was greater than that in a bath not containing aluminum. On the other hand, aluminum in steel had no effect on the galvanizing reaction. He indicated that at least 0.2 to 0.3 per cent aluminum is required for control of the growth of the iron-zinc alloy layer. Also, he suggested that inhibition might be associated with a preferential iron-aluminum reaction which caused the formation of characteristic blue-gray crystals.

The literature prior to 1950 was reviewed independently by Thorley[2] and Hughes.[3] The review by Hughes specifically covered the effects of aluminum and served as an introduction to his work, whereas Thorley covered the general galvanizing literature. Both authors

indicate the conflicting reports at that time concerning the amount of aluminum required to minimize iron-zinc alloy layer growth. Aluminum levels quoted ranged from 0.1 to 0.3 per cent. Disagreement for the optimum aluminum level, however, was attributed to differences in experimental conditions such as bath temperature, immersion time, bath composition (other than aluminum content) and base metal composition.

Hughes indicated that the aluminum level necessary to limit iron-zinc alloy layer growth was dependent on bath temperature and immersion time. He also described in this and another paper[4] the various theories of alloy layer inhibition which were suggested at the time. These included Rowland's "aluminum oxide membrane theory", Bablik's "induction period theory" and Hall and Kentworthy's "loose alloy theory." Hughes subsequently described experiments which apparently disproved each of these proposed theories. Instead, based on chemical analysis and X-ray diffraction results obtained for coatings prepared in a bath containing 1.5 per cent aluminum, he proposed that a ternary iron-zinc-aluminum layer which formed at the steel interface inhibited the growth of iron-zinc alloy layers. Hughes' work was done at temperatures from 430°C to 490°C, apparently in high iron baths with air cooling.

In 1952, Haughton,[5] in carefully controlled experiments, found a film of Fe_2Al_5 on the surface of the steel after stripping coatings containing 0.1 to 0.2 per cent aluminum in a 5 per cent sulfuric acid solution with arsenious oxide for an inhibitor. He proposed that this

very thin layer of Fe_2Al_5, rather than the ternary layer suggested by Hughes, prevented attack by zinc. The Fe_2Al_5 layer was identified by the X-ray powder method and its thickness was estimated to be 0.0002 mm as measured by taper microsection. Haughton also showed that formation of the inhibiting Fe_2Al_5 layer was limited by high iron contents in the bath, rough steel surfaces, and unagitated baths. Haughton's work was done at 450°C in pure zinc baths containing 0 to 0.2 per cent aluminum and the iron content was varied from about 0.002 per cent to saturation. Specimens were coated with and without agitation for 1 and 5 minutes and quenched in water after coating.

In the discussion of Haughton's paper, Bablik[6] indicated that he had also suggested the formation of an iron-aluminum layer (Fe_3Al) which inhibited iron-zinc alloy growth. He indicated that this iron-aluminum layer subsequently underwent a transformation, possibly a lattice rearrangement, which promoted rapid attack and thick iron-zinc alloy layers.

Horstmann[7] investigated the effects of 0.1 to 0.5 per cent aluminum on still and agitated specimens in iron saturated baths at temperatures from 440°C to 500°C. He established, from iron loss measurements, the minimum aluminum content necessary for inhibition as a function of temperature. He also made surface X-ray diffraction analyses on inhibited 0.5 per cent aluminum coatings and confirmed the presence of Fe_2Al_5. In addition, he examined a partially inhibited coating and found lines for Fe_2Al_5, FeAl and other indistinct lines

which were assumed to be associated with a ternary iron-zinc-aluminum compound. Thus, Horstmann proposed that a protective layer of Fe_2Al_5 initially forms on the surface of the iron which prevents access of the zinc bath to the iron. Like Bablik, he suggested that after a certain time this Fe_2Al_5 layer reacts with the bath and transforms to other iron-aluminum and iron-zinc-aluminum compounds which lead to increased iron attack and alloy layer growth.

Sebisty and Edwards[8] studied the effect of aluminum on coating properties and the loss of iron from the steel base. However, they did not discuss the mechanism by which aluminum suppresses alloy growth nor did they identify any intermediate aluminum-rich alloy layer.

Cameron and Ormay[9] studied the effect of aluminum, mainly from 0 to 0.5 per cent, at 440°C to 450°C for immersion times from five seconds to two hours with and without bath agitation. In addition, the iron content of the bath, base steel composition and cooling rate were studied. Identification of the various phases was made mainly by metallographic examination and microhardness measurements, along with some incomplete X-ray diffraction and electron-probe microanalyses. They made definite X-ray diffraction identification of Fe_2Al_5 and identified aluminum-bearing delta ($FeZn_7$) which, they stated, had lines similar to those for the ternary compound reported by Horstmann. Other phases reported to be present under various conditions were aluminum-bearing

zeta ($FeZn_{13}$), $FeAl_3$ and a ternary compound.

Based on this work, they presented a schematic ternary activity diagram which indicates the iron-zinc and iron-aluminum phases which may form as a function of aluminum content and bath agitation. They suggest for baths containing about 0.25 per cent aluminum that an induction period occurs in which parts of the steel surface are dissolving but at isolated areas iron-aluminum layers nucleate and grow, eventually covering the surface. However, localized depletion of aluminum below 0.15 per cent causes rapid growth of iron-zinc compounds. As a result, they suggest that aluminum layers are favored by agitation and short immersion times whereas, static conditions and long times favor zinc phases. Thus, at intermediate aluminum levels, aluminum phases form initially but are later transformed to zinc phases.

As indicated, investigators studying the effect of aluminum in galvanizing baths have reported the presence of an iron-zinc-aluminum ternary compound in the coating. In fact, Cameron and Ormay[10] constructed a tentative section of the zinc-rich corner of the zinc-aluminum-iron system which included a ternary compound. However, no ternary compound has ever been reported by investigators studying the zinc-aluminum-iron system.

No ternary compound is shown in the ternary diagram reported in the Compendium of Constitutional Ternary Diagrams of Metallic Systems[11] which was prepared by the U. S. Air Force, and which is based on work by

Mondolfo, Moyer, Schram, Raynor and Gebhardt. Raynor, et al,[12] and Gebhardt[13] both found that $FeAl_3$ was in equilibrium with zinc-rich melts. Also, both found no evidence for a ternary compound in the system. Rennhack[14] also studied the zinc-rich corner of the diagram and found no evidence for a ternary compound. He did indicate, however, that $FeZn_7$ (delta) is in equilibrium with Fe_2Al_5 and $FeAl_2$, whereas $FeZn_{13}$ (zeta) is not in equilibrium with iron-aluminum compounds. He also reported that about 0.2 per cent aluminum is soluble in $FeZn_{13}$ at 450°C. His diagram shows the convergence of a number of phase fields, which involve zinc with iron-aluminum and iron-zinc compounds. Thus, he concluded that more work is required adjacent to the zinc vertex to locate the phase boundaries precisely.

Finally, Southin and Wright[15] made an interesting observation in studying the effect of small concentrations of aluminum (0.3 per cent) and iron (0.05 per cent) in high purity zinc used for sacrificial anodes in cathodic protection. They reported the presence of crystals of Fe_2Al_5 in this alloy, as identified by X-ray diffraction. They concluded that none of the work on the ternary system predicts that Fe_2Al_5 would be formed in such an alloy. However, this work shows the persistence of this phase in zinc containing iron and aluminum and the high reactivity of iron and aluminum towards each other in zinc melts.

MATERIALS

Zinc

New Jersey Zinc Company "Horsehead" Special High Grade Zinc was used. The composition of this zinc meets the ASTM Specification B6-58 for Slab Zinc (Spelter) which gives the following composition limits:

Lead	- 0.006 max, per cent
Iron	- 0.005 max, per cent
Cadmium	- 0.004 max, per cent
Sum of Lead, Iron and Cadmium	- 0.010 max, per cent

Steel

Cold rolled steel sheet of 24 gage was used. The chemical analysis of the steel was as follows:

C	Mn	P	S	Si	Ni	Cr	Mo	Cu	Al
0.06	0.47	0.006	0.023	<0.01	0.01	0.04	<0.01	<0.02	0.006

Aluminum

Additions of aluminum were made with aluminum ingot of 99.50% minimum purity. The chemical analysis was as follows:

Aluminum	- 99.82 per cent
Iron	- 0.06 per cent
Silicon	- 0.10 per cent

Iron

Low iron bath contents were controlled by the iron impurity levels in the zinc and aluminum and by the build-up from attack on the steel during galvanizing. The intermediate iron contents were achieved by dissolving

pure iron wire in the bath at the coating temperature. The wire contained 99.91 per cent iron and was 0.009 inches in diameter.

COATING PROCEDURE

A sequential procedure was used in conducting this work. The coating method was consistent throughout the test; however, there was some slight variation in the specimen configuration, the number of specimens coated for a given condition and the number of baths used for a given coating composition. These variations were made necessary as data were developed for coatings made in low iron, 0.30 per cent aluminum baths and eventually led to a standardized procedure for the 0.20 per cent aluminum baths. These slight variations in procedure, however, did not significantly affect the results for the 0.30 per cent aluminum baths.

Galvanizing Bath

A Lindberg Model CR-5 crucible furnace was used with a Norton Crystalon G ceramic pot 7-1/4 inches deep and 3-3/4 inches inside diameter. Approximately 15 pounds of zinc were used which filled the pot to about the 6-inch level.

Bath Compositions

Aluminum compositions investigated were about 0.20 and 0.30 per cent. At 0.20 per cent aluminum, both a low iron level of about 0.003 per cent and an intermediate iron level of about 0.012 per cent were investigated. However, only a low iron level of about 0.005 per cent was investigated for 0.30 per cent aluminum baths. The iron content increased slightly during dipping because iron entered the bath from each specimen dipped.

The 0.012 per cent iron level is designated intermediate because saturation is about 0.03 per cent iron at 450°C.

Immersion Temperatures and Times

Immersion temperatures studied for each bath composition were as follows:

430°C
450°C
470°C

The bath temperature was monitored before and after each specimen was dipped using a Chromel-Alumel thermocouple with a Leeds and Northrup Model 8657-C Double Range Potentiometer Indicator. The bath temperature during dipping of each specimen was within ± 5°C of the aim temperatures.

The following immersion times were studied for each bath composition:

20 seconds
40 seconds
80 seconds
160 seconds
320 seconds

Preparation of Specimens

An open corner box section specimen was used. This configuration was adopted to give a maximum coated surface area which could be conveniently dipped into the bath and to minimize cut edge effects. Preliminary tests made on individual panels, 1 inch x 3-1/2 inches, showed that rapid alloy growth at cut edges significantly affected the weight of alloy results.

Figure 1 is a sketch showing the dimensions and configuration of the box section. As shown, the two closed sides were 2-1/2 inches wide and the two open sides were 1-1/2 inches wide. The length of the section was 4 inches. A galvanized soft iron wire handle which was crimped through 1/4 inch diameter holes on opposite corners was used to support the section. The open corner gave free access of the bath to the inside surfaces of the section.

Triplicate sections were coated for each condition for the 0.30 per cent aluminum bath and duplicate sections were coated for 0.20 per cent aluminum baths.

After being sheared and having the holes punched, flat 4 inches x 8 inches sheet samples were formed into the box sections on a brake. The supporting wires were then attached and the sections were degreased in trichlorethylene vapor. The sections were then pickled for 15 seconds in a 10 per cent hydrochloric acid solution at about 82°C. After pickling, the sections were rinsed in hot running water and fluxed for 30 seconds in a 280 grams/liter solution of DuPont Zaclon F galvanizing flux, which was also at about 82°C. The sections were then dried in an oven at about 50°C prior to dipping.

Dipping Procedure

After fluxing, the sections were dipped for each indicated immersion time, quickly hand withdrawn from the bath and air-cooled to room temperature. The sections were hand held during dipping and were agitated in the bath in a gentle reverse circular motion about a vertical axis and occasionally moved vertically up and down under the bath surface. The

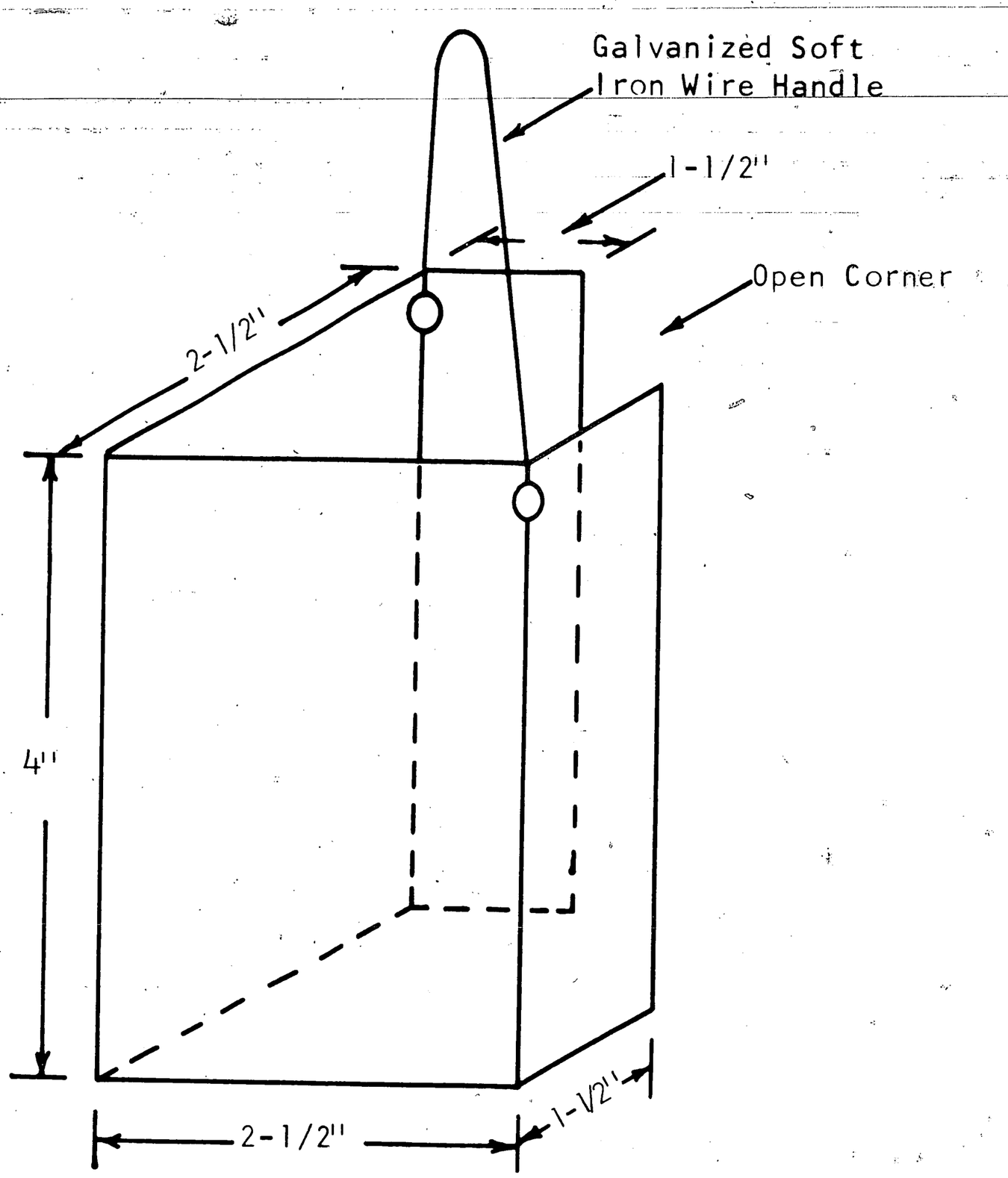

FIGURE 1. Configuration of Box Section Specimen.

bath was skimmed of oxide before dipping and before withdrawing the section from the bath.

Bath samples were usually taken at the beginning, middle and end of the time series for each particular temperature. The iron and aluminum contents were then determined by chemical analysis.

Initially, for the 0.30 per cent aluminum composition, a single bath was used to coat box section specimens for each time at all three temperatures. Later, separate baths were prepared for each of the three temperatures to minimize the amount of iron entering the bath from the specimens and to ensure that the iron level remained low. This latter procedure was also adopted for the low iron level, 0.20 per cent aluminum composition baths. In these baths, the low iron level compositions were prepared first for each temperature. Then, the iron content for that particular bath was raised to the intermediate level by making additions of pure iron wire. Thus, four baths were prepared for the 0.30 per cent aluminum composition and three baths for the 0.20 per cent aluminum composition.

Sampling

Coated box sections were cut with a saw along the three corners to give two panels 2-1/2 inches x 4 inches and two panels 1-1/2 inches x 4 inches for each section. Next, one specimen 1 inch x 3-1/2 inches was sheared from each 2-1/2 inches x 4 inches panel to give duplicate specimens for weight of alloy measurements. These specimens were sheared

such that cut edges exposed in the bath during coating were removed. Three, 1 inch x 2 inches specimens were then sheared from near the centers of the remainder of these panels for metallographic examination, X-ray diffraction analysis and electron microscope examination. The two 1-1/2 inches x 4 inches panels were held in reserve.

WEIGHT OF ALLOY PROCEDURE

The weight of the inhibiting aluminum rich alloy layer was determined by a combination method employing the stripping technique used by Haughton[16] to remove the zinc overlay and a method reported by Ikenberry[17] to remove the iron-aluminum alloy layer on aluminum coatings.

Briefly, Haughton reported that coatings containing up to 0.05 per cent aluminum were stripped bright and clean in the 5 per cent solution of sulfuric acid containing 2 grams/liter of arsenious oxide, But, those coatings containing from 0.1 to 0,2 per cent aluminum were coated with an adherent dark film after stripping. He later identified this film as Fe_2Al_5. Thus, this particular stripping solution attacks zinc and iron-zinc phases but does not attack aluminum-rich phases.

The method reported by Ikenberry is for determining the relative weights of the aluminum overlay and iron-aluminum alloy layer on aluminized coatings. In this method, the iron-aluminum alloy layer is removed in a hot solution of 20 per cent sodium hydroxide after the aluminum overlay is removed in a stannous choride solution. Thus, hot caustic solutions readily attack iron-aluminum phases without significant attack of the steel base.

Accordingly, the following method was used to determine the weight of the inhibiting aluminum-rich alloy layer. Note that specimens were handled by the edges throughout the entire procedure.

(a) The length and width of the 1 inch x 3-1/2 inches specimens were measured to the nearest 0.1 millimeter using a Glogau No. 12 vernier caliper. The area in square millimeters was then calculated. The specimens were then degreased in trichlorethelyene vapor.

(b) The zinc overlay was removed by immersing the specimens in a 5 per cent sulfuric acid solution with 2 grams/liter of sodium arsenite until there was no visible reaction. (Sodium arsenite was used because it is more soluble in this acid solution and it gives the same result as arsenious oxide). The specimens were then washed in warm running water, immersed in methanol and dried with compressed air. Next, the specimens were given a flash immersion in cold concentrated nitric acid to remove the residual arsenic film, quickly rinsed again in warm running water, followed by another methanol rinse, dried and desiccated. The specimens were then weighed to the nearest 0.001 milligram on a Mettler M-5 micro balance.

(c) The iron-aluminum alloy layer was removed by immersing the specimens in a hot solution of 20 per cent sodium hydroxide until the action stopped. Then, the specimens were rinsed in warm running water, immersed in methanol and dried. Next, the specimens were given a flash immersion in cold concentrated

hydrochloric acid to remove the smut, quickly rinsed in water, then in methanol and dried. The specimens were again weighed on the micro balance and the weight of the aluminum-rich alloy layer was determined by the difference in weight before and after stripping. Finally, the weight of alloy was calculated in terms of grams/square meter.

PHASE IDENTIFICATION TECHNIQUES

Preparation of Metallographic Specimens

Specimens about 3/8 inch x 1 inch were sheared from the specimen set aside for metallographic examination. Five specimens of each time series were then mounted in Bakelite. Next, coarse grinding was done using water on a slow speed Buehler wet surfacer through the following grit papers: 120, 240, 320, 400 and 600. Water rinsing was not used after this stage to avoid staining.

Polishing was done by hand using diamond polishing compound. Cleaning and rinsing between polishing steps was done in ethyl alcohol in a sonic cleaner. First, coarse polishing was done on Texmet cloth (no nap and with an adhesive backing) on a glass backing plate using 6 micron diamond polishing compound with AB Metadi oil lubricant. Then, final polishing was done on Buehler Microcloth on a glass backing plate using 1 micron diamond dust compound with AB Metadi oil lubricant.

Finally, the specimens were etched for 10 to 15 seconds in 2 to 3 per cent nitric acid in amyl alcohol, followed by rinsing in ethyl alcohol in a sonic cleaner.

Electron-Probe Microanalysis

Specimens used for electron-probe microanalysis were the same specimens used in the metallographic examinations. A Cambridge, Model Mark-Two, "Microscan" electron-probe microanalyser was used.

The usual techniques were employed in making slow-scan electron plots and radiation scanning images. Selected point analyses were also made by comparing intensities of pure standards of iron, zinc and aluminum with the intensity of these same elements in the coating.

X-Ray Diffraction Analysis

The zinc overlay on the 1 inch x 2 inches specimens was stripped to expose the aluminum-rich alloy layer prior to making the X-ray diffraction analysis. Stripping was done in the 5 per cent sulfuric acid overlay stripping solution, followed by the flash concentrated nitric acid rinse. Only coatings immersed for 20 and 320 seconds for each bath temperature and bath composition were analyzed.

A General Electric XRD-5 X-ray Diffractometer was used to make the analysis. The unit was equipped with a special holder for mounting a 1 inch x 2 inches sheet specimen which enabled a slow surface scan to be made from 24 to 145 degrees. The instrument conditions were as follows:

Tube - Chromium Target at 50 KVP at 32 ma.
Filter - Vanadium
Take Off Angle - 4 degrees
Beam Slit - 3 degrees
Soller Slit - Medium Resolution
Detector Slit - 0.2 degrees
Scan Rate - 0.2 degrees/minute
Time Constant - 8 seconds
Counter Tube - Dual, #7 and #6
Recording Scale - 200 cps Linear
Chart Speed - 6 inches/hour

Electron Microscope Examination

The surface of the aluminum-rich alloy layer was exposed by stripping the zinc overlay in the sulfuric acid overlay stripping solution and nitric acid flash rinse solution prior to making the electron microscope analysis. Again, only the 20 and 320 seconds specimens for each bath temperature and bath composition were examined.

A two-stage, pre-shadowed carbon replica method was used to examine these specimens. First a 1.5 mil coating of cellulose acetate was applied by dissolving acetate with acetone on the surface of the specimen. This cellulose acetate coating was then dry stripped by hand. Next, platinum-palladium (80-20) was evaporated onto the cellulose acetate surface replica at an angle of about 16 degrees, followed by evaporation of carbon. The replica was then placed onto a 200 mesh copper grid, 1/8 inch x 1/8 inch, and lowered into acetone to dissolve the cellulose acetate film, thereby giving a positive carbon replica.

An RCA Model EMU-3E electron microscope was used to make these examinations. Electron gun power supplies of both 50 and 100 KVA were used.

EXPERIMENTAL DATA

Coating Bath Chemical Analyses

Chemical analyses of the coating baths for the following aim compositions are shown in Tables I and 2.

a) 0.30 per cent aluminum, 0.004 per cent iron
b) 0.20 per cent aluminum, 0.004 per cent iron
c) 0.20 per cent aluminum, 0.013 per cent iron

The actual bath compositions were well within the aim compositions. The iron level, however, did increase for the low iron baths at 470°C owing to the iron entering the bath during dipping.

Notice that two sets of chemical analyses are shown for 0.30 per cent aluminum composition baths in Table I. The original bath was a single bath used to coat duplicate box sections for all immersion times at all temperatures. In a subsequent test, separate baths were prepared for each temperature and a single box section was coated for each immersion time. Thus, four coating baths were prepared for the 0.30 per cent aluminum composition and triplicate box sections were available.

This same separate bath procedure was followed for the 0.20 per cent aluminum baths, except that the same bath was used for both the low and intermediate iron levels at each temperature. Thus, three coating baths were prepared for the 0.20 per cent aluminum composition and duplicate box sections were made for each immersion time.

Modification of the procedure was brought about by results obtained for the original bath for the 0.30 per cent aluminum composition. There

TABLE I

CHEMICAL ANALYSES FOR 0.30 PER CENT ALUMINUM BATHS

Original Bath (Low Iron)
(Single bath used for all coating temperatures)

	430 °C		450 °C		470 °C	
	Wt. % Al	Wt. % Fe	Wt. % Al	Wt. % Fe	Wt. % Al	Wt. % Fe
START	0.30	<0.01	0.30	<0.01	0.31	<0.01
MIDDLE	-	-	-	-	-	-
END	0.29	<0.01	0.30	<0.01	0.29	<0.01

Separate Baths (Low Iron)
(Separate bath used for each temperature)

	430 °C		450 °C		470 °C	
	Wt. % Al	Wt. % Fe	Wt. % Al	Wt. % Fe	Wt. % Al	Wt. % Fe
START	0.31	0.004	0.32	0.004	0.34	0.004
MIDDLE	0.32	0.004	0.32	0.004	0.32	0.005
END	0.31	0.004	0.32	0.004	0.32	0.006

TABLE 2

CHEMICAL ANALYSES FOR 0.20 PER CENT ALUMINUM BATHS

Low Iron Bath*

	430 °C		450 °C		470 °C	
	Wt. % Al	Wt. % Fe	Wt. % Al	Wt. % Fe	Wt. % Al	Wt. % Fe
START	0.22	0.002	0.22	0.002	0.22	0.001
MIDDLE	0.22	0.003	0.21	0.003	0.22	0.003
END	0.21	0.004	0.21	0.004	0.22	0.007

Intermediate Iron Bath*

	430 °C		450 °C		470 °C	
	Wt. % Al	Wt. % Fe	Wt. % Al	Wt. % Fe	Wt. % Al	Wt. % Fe
START	0.21	0.014	0.21	0.012	0.21	0.011
MIDDLE	0.20	0.012	0.21	0.014	0.21	0.012
END	0.20	0.013	0.21	0.015	0.20	0.014

* Separate baths were used for each temperature. However, the same bath was used for both low and intermediate iron levels for each corresponding temperature.

was a question whether the results may have been affected by the iron entering the bath during dipping. Thus, the additional separate baths for each temperature were made to minimize iron pick-up, thereby ensuring that low iron levels would be maintained.

Finally, notice from Table I that iron was analyzed to the nearest 0.001 per cent after results were obtained on the original bath for the 0.30 per cent aluminum composition. As the results indicate, this accuracy is required.

Microstructures of Coatings

Coatings containing 0.2 and 0.3 per cent aluminum consist mainly of a zinc overlay with essentially no alloy layer for all immersion temperatures at all immersion times. Typical photomicrographs for 0.2 and 0.3 per cent aluminum coatings at 450°C and 80 seconds immersion time are shown in Figure 2. There is no visible alloy layer at the zinc-steel interface for either the 0.2 and 0.3 per cent aluminum coatings. Thus, the usual duplex iron-zinc alloy layers normally present on zinc coatings are inhibited in aluminum-bearing coatings. These micro-sections are also representative of coatings made at 430°C and 470°C for all immersion times.

Although growth of iron-zinc alloy layers was essentially suppressed in these coatings, there were areas of rapid, localized alloy layer growth where inhibition apparently breaks down. Figure 3 shows localized alloy layer growth on a 0.3 per cent aluminum coating which was coated at 470°C for an immersion time of 160 seconds. Notice that the growth is burst-like with adjacent areas showing no attack. Growth was shallow and particles apparently were sloughing off into the bath. The color of the particles was blue-gray.

Localized growths on 0.2 per cent aluminum coatings with intermediate iron contents at temperatures of 430°C and 470°C are shown in Figure 4. Notice the difference in the nature of the growth between the 430°C and 470°C. The 430°C coating shows a shallow duplex layer which apparently sloughs off into the bath. But the 470°C coatings show deep-seated duplex

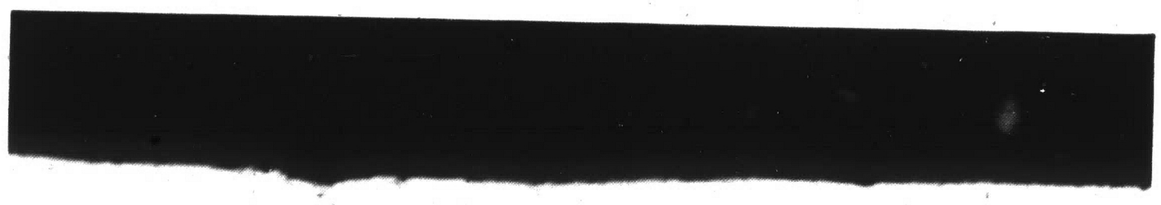

a) 0.21% Al, 0.014% Fe
450°C, 80 second immersion

b) 0.32% Al, 0.004% Fe
450°C, 80 second immersion

FIGURE 2. Typical cross-sections of 0.2 and 0.3 per cent aluminum coatings. 500X. Nitric acid-amyl alcohol etch.

The coatings consist mainly of a zinc overlay with no visible alloy layer growth at the zinc-steel interface.

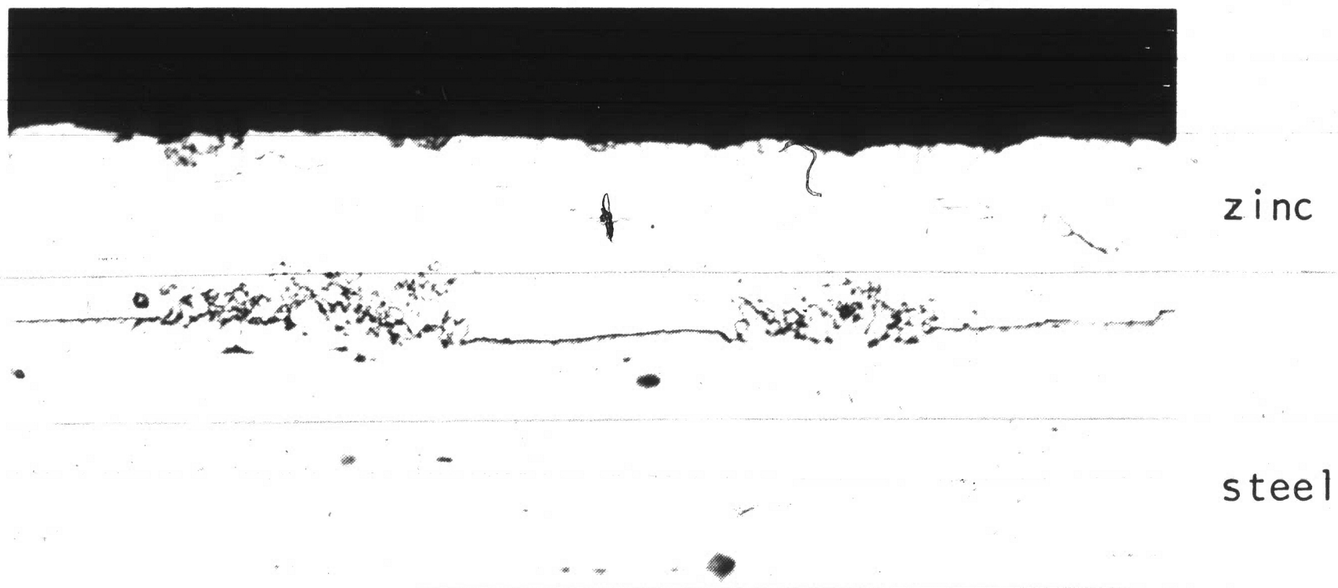

FIGURE 3. Localized alloy growth on a 0.32 per cent aluminum coating with 0.006 per cent Iron which was made at 470° C with a 160 second immersion. 500 X. Nitric acid-amyl alcohol etch.

Growths are burst-like with adjacent areas showing no attack. The particles were sloughing off into the bath and their color was blue-gray.

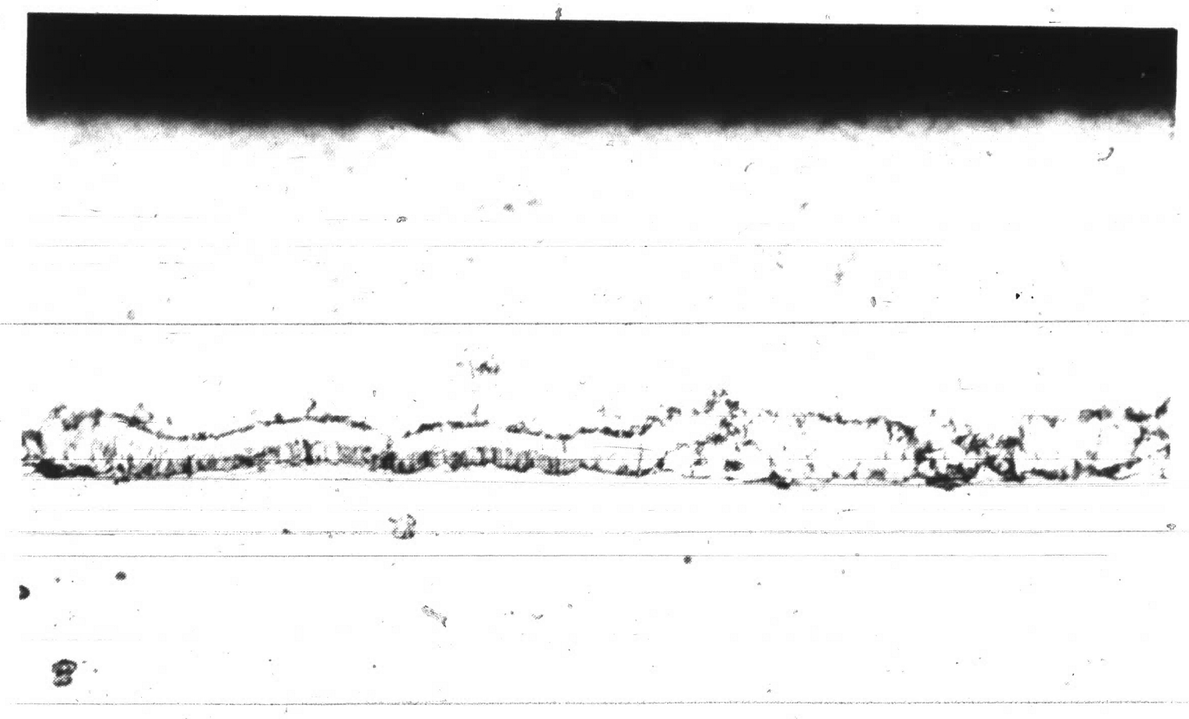

a) 0.20% Al, 0.013% Fe
430°C, 320 seconds immersion

b) 0.20% Al, 0.014% Fe
470°C, 320 seconds immersion

FIGURE 4. Localized Alloy Growth on 0.2 per cent Aluminum Coatings made at 430°C and 470°C. 500X. Nitric acid-amyl alcohol etch.

Shallow duplex alloy growth occurred at 430°C, whereas deep-seated duplex growth with adjacent blue-gray particle growth occurred at 470°C.

growths with adjacent areas of blue-gray particle growths similar to that on the 0.3 per cent aluminum coatings. Haughton[18] observed similar deep-seated growths on 0.2 per cent aluminum coatings made in baths low in iron.

Summarizing, baths containing 0.2 and 0.3 per cent aluminum generally inhibit attack by zinc. However, random localized alloy growth occurs which leads to the formation of iron-zinc phases. The frequency of this localized alloy growth seems to increase as

1) the temperature is increased
2) the immersion time is increased
3) the aluminum is decreased, and
4) the iron is increased.

Electron-Probe Microanalysis

An electron-probe microanalysis of these coatings confirms that aluminum is, indeed, concentrated at the zinc-steel interface. Figure 5 shows the results of this analysis for a 0.22 per cent aluminum coating with 0.013 per cent iron which was made at 430°C with an 80 second immersion. The area shown in the electron back-scatter scanning image is typical of those shown in Figure 2 in which no apparent alloy layer is visible at the zinc-steel interface. The change in concentration of aluminum, zinc and iron through the interface is shown in the slow scan plots along the line indicated on the electron scanning image. These slow scans clearly show that aluminum is highly concentrated at the interface, whereas the zinc and iron concentrations decrease and increase respectively at this interface.

Figure 6 shows a similar analysis made on a 0.30 per cent aluminum coating with 0.004 per cent iron which was made at 430°C with a 20 second immersion. An X-ray scanning image for aluminum $K\alpha$ is also included for this area with the slow scan for aluminum. Again, aluminum is concentrated at the interface as shown by the peak in the slow scan and the bright area on the X-ray image. Similar results were obtained for all other coatings with 0.2 and 0.3 per cent aluminum at areas which showed no visible alloy layer growth at the zinc-steel interface.

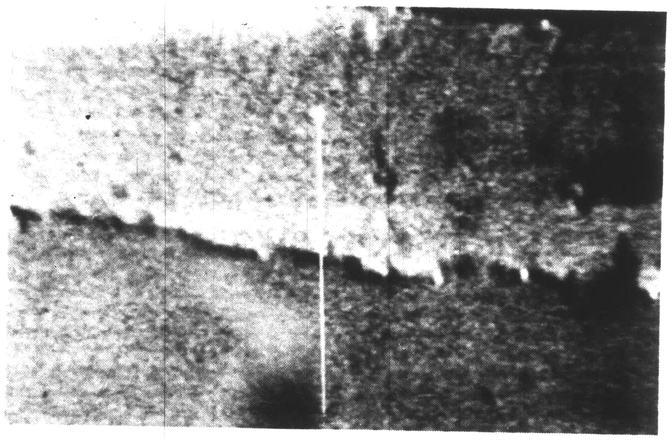

zinc

steel

Electron Scanning Image

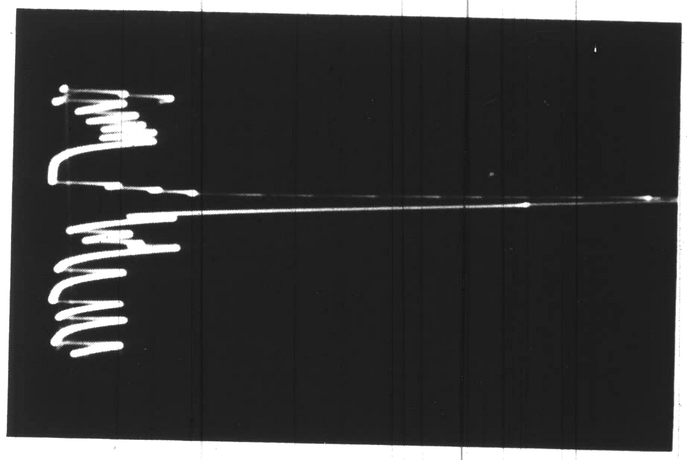

Aluminum Slow Scan 100 cps

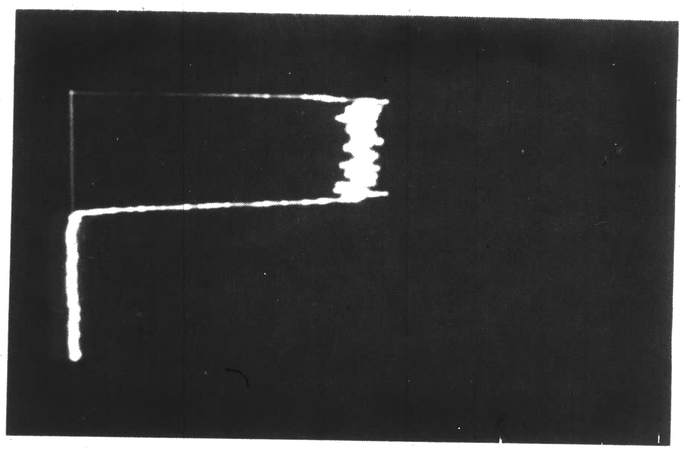

Zinc Slow Scan 30,000 cps

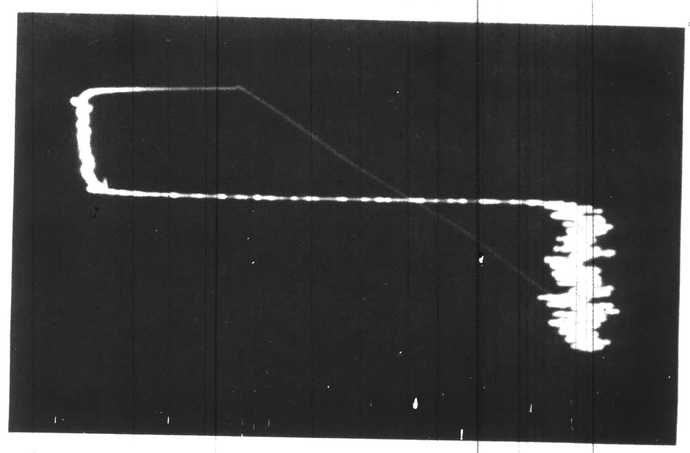

Iron Slow Scan 30,000 cps

FIGURE 5. Electron-Probe Microanalysis of a 0.22 Per Cent Aluminum Coating Containing 0.013 Per Cent Iron which was made at 430°C with an 80 Second Immersion. 500 X.

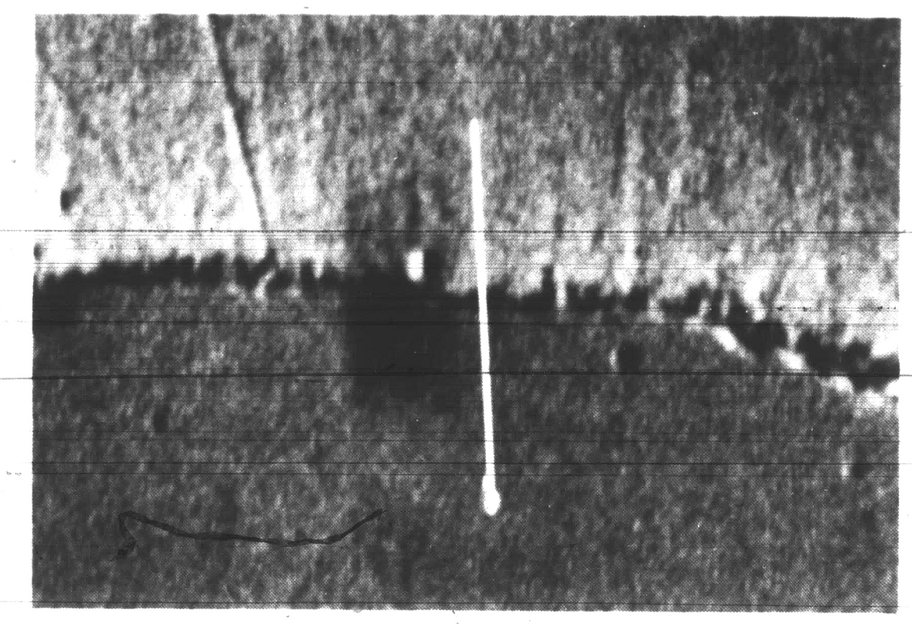

zinc

steel

Electron Scanning Image

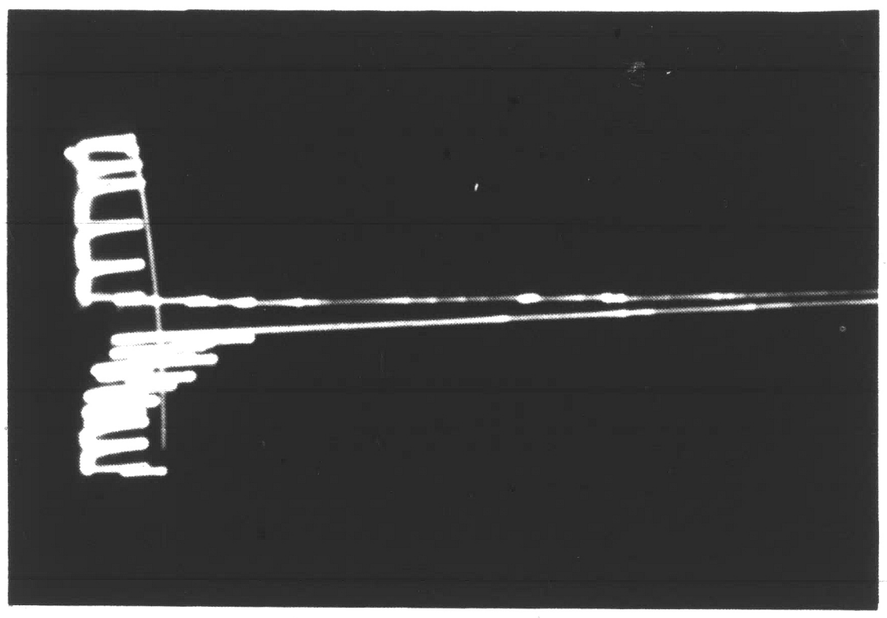

Aluminum Slow Scan 300 cps

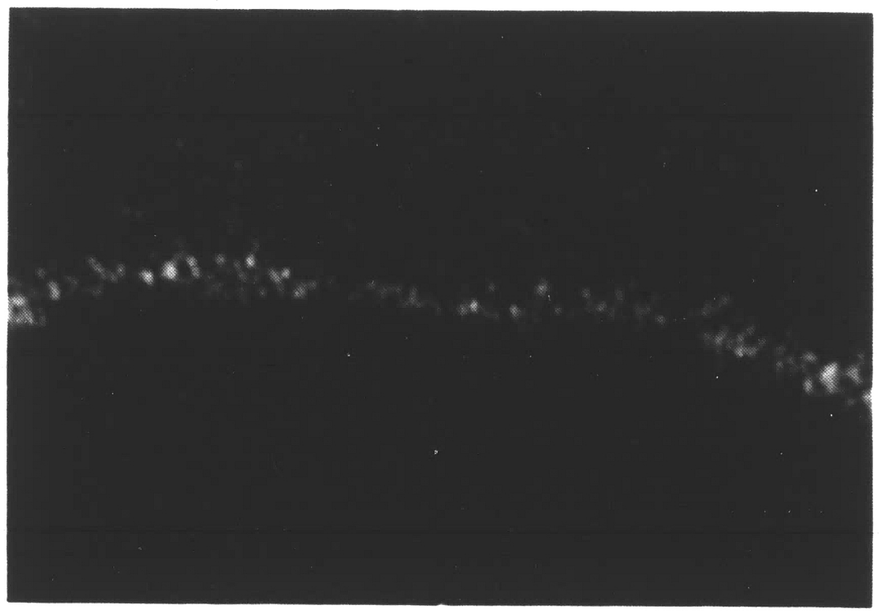

zinc

steel

Aluminum K∝ Radiation Image

FIGURE 6. Electron-Probe Microanalysis of a 0.30 Per Cent Aluminum Coating Containing 0.004 Per Cent Iron which was made at 430°C with a 20 Second Immersion. 750X

Weight of Alloy Data

During preliminary work, various methods were tried to measure or weigh the aluminum-rich alloy layer in addition to the sulfuric acid-sodium hydroxide stripping method. These methods included a taper microsection technique similar to that used by Davies and Hoare[19] to measure the iron-tin alloy layer on tinplate, an anodic stripping method in a weak sodium hydroxide solution similar to that reported by Kunze and Willey[20] also for tinplate, and the stannous chloride method reported by Ikenberry[21] for aluminized coatings. Each method had associated difficulties which gave less accurate thickness or weight measurements than the sulfuric acid-sodium hydroxide stripping method; therefore, none were used in this work. There were, however, indications that the anodic stripping technique might be made adaptable with some additional effort.

As mentioned earlier, Haughton reported that the sulfuric acid-arsenite stripping solution attacked iron-zinc phases but not aluminum-rich phases. To confirm this and to determine what phases at the alloy layer were being weighed, coatings stripped of the zinc overlay in the sulfuric acid-arsenite solution were electroplated with copper and examined metallographically. Electroplating with copper preserves the interface during polishing and shows the phases present after stripping. (Details concerning the electroplating method are described in the appendix).

Figure 7 shows photomicrographs of electroplated copper coatings on zinc overlay stripped coatings containing about 0.2 per cent aluminum and about 0.012 per cent iron which were made at 450°C and 470°C with a 320 second immersion time. Note that an extremely thin layer is present at the interface with the blue-gray particles previously observed in Figure 4b. No localized bursts of iron-zinc phases were present on any of these stripped coatings which were electroplated with copper. Thus, the total weight of alloy measured after stripping in the hot sodium hydroxide solution is comprised of the weight of the thin layer at the interface and the weight of the aluminum-rich blue-gray phase.

Complete weight of alloy data for each bath composition are shown in Tables 3, 4, and 5. Included are the area and weight of alloy for each individual specimen for each coating temperature and immersion time. The average weight of alloy in terms of grams per square meter for each bath composition, coating temperature and immersion time is summarized in Table 6. Note that the weight of the alloy layer ranges from about 0.4 to 3.5 grams per square meter. The usual total coating weight for continuously applied galvanized coatings is about 382 grams per square meter (1.25 ounces per square foot). Thus, the weight of this alloy layer is only about 0.1 to 0.9 per cent of the total weight of the coating. Assuming for now that the layer is mostly Fe_2Al_5* and expressing the weight in terms of thickness, this alloy layer thickness ranges from about 0.1 to 0.8 micron (0.004 to 0.033 mil). Or, comparison with the equally familiar tinplate coatings shows that the lighter weights of alloy are about the order of thickness of the $FeSn_2$ alloy layer or about 0.15 micron (0.005 mil).

---

* The density for Fe_2Al_5 was calculated to be 4.21 grams per cubic centimeter from X-ray data.

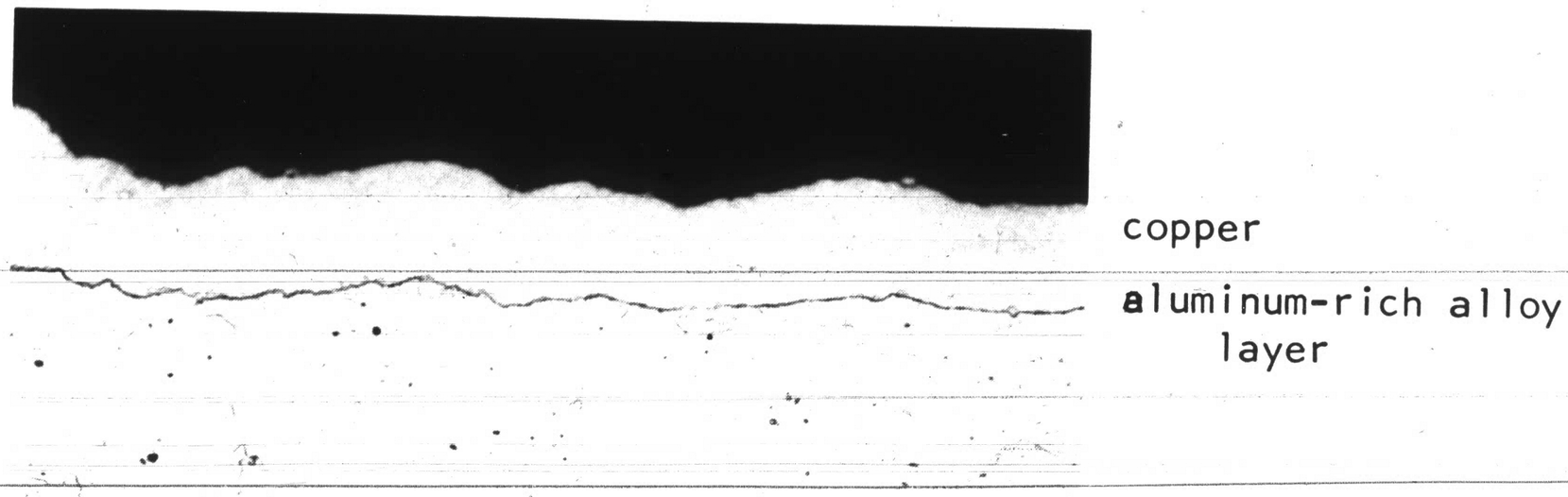

a) 0.21% Al, 0.015% Fe
450°C, 320 seconds immersion

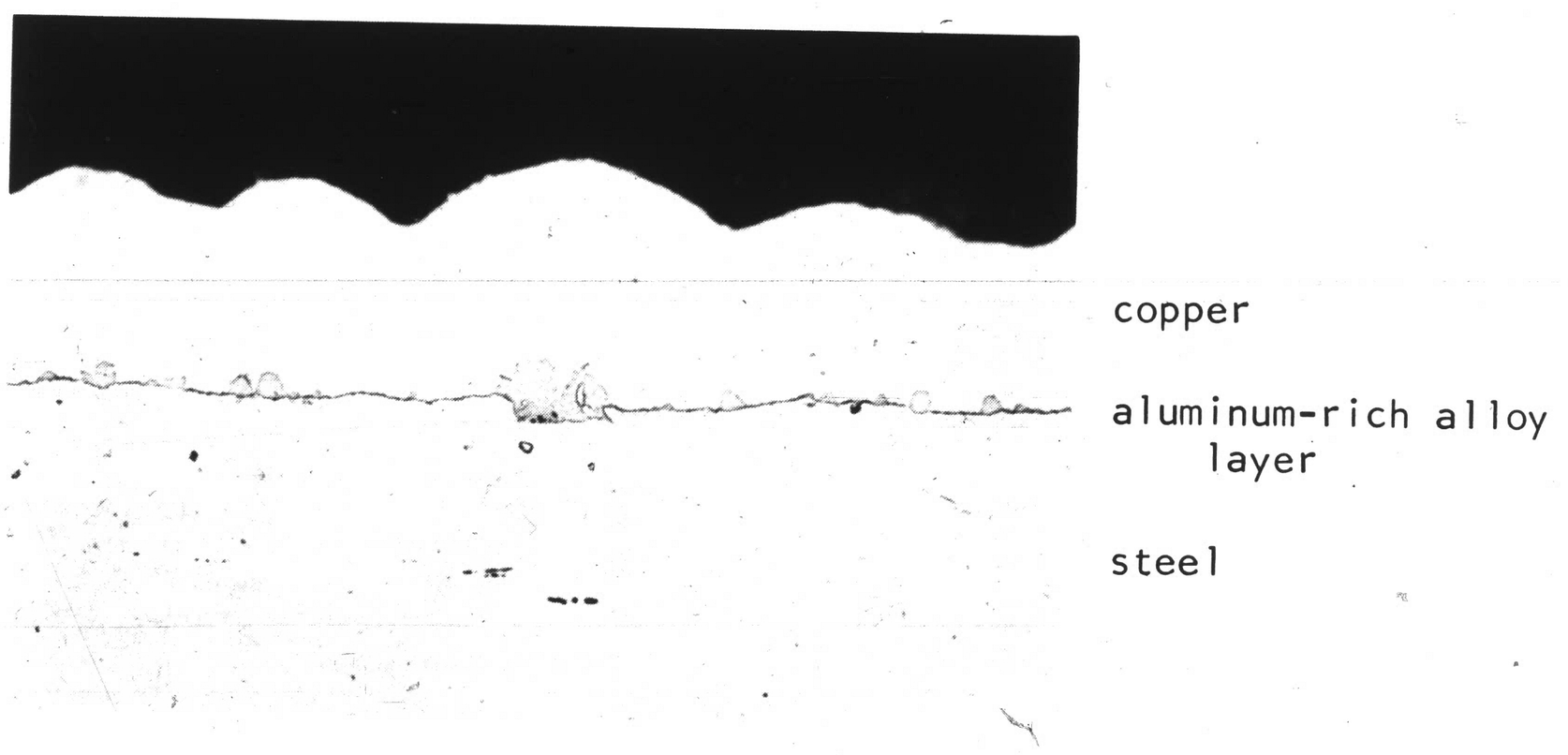

b) 0.20% Al, 0.014% Fe
470°C, 320 seconds immersion

FIGURE 7. Coatings Stripped of the Zinc Overlay and Electroplated with Copper to Preserve the Interface. 500X
Nitric Acid-Amyl Alcohol Etch.

A very thin layer and particles of blue-gray phase are present after stripping with the sulfuric acid-arsenite solution.

TABLE 3

WEIGHT OF THE ALUMINUM-RICH ALLOY LAYER ON ZINC COATINGS CONTAINING ABOUT 0.20 PER CENT ALUMINUM WITH 0.002 TO 0.007 PER CENT IRON DETERMINED BY THE SULFURIC ACID-SODIUM HYDROXIDE WEIGH-STRIP-WEIGH METHOD

Sample Number	Temperature °C	Immersion Time Seconds	Area (Both Sides) sq. mm.	Weight of Alloy Layer mg	Weight g./sq. m.	Average g./sq. m.
140A	430	20	4506.0	3.465	0.769	
B	430	20	4478.1	3.219	0.719	0.771
141A	430	20	4470.5	3.522	0.788	
B	430	20	4511.0	3.640	0.807	
142A	430	40	4488.2	3.382	0.754	
B	430	40	4523.7	3.250	0.718	0.731
143A	430	40	4483.2	3.194	0.712	
B	430	40	4506.0	3.331	0.739	
144A	430	80	4483.2	3.945	0.880	
B	430	80	4493.3	3.877	0.863	0.811
145A	430	80	4447.7	3.233	0.727	
B	430	80	4506.0	3.489	0.774	
146A	430	160	4506.0	3.133	0.695	
B	430	160	4506 0	3.185	0.707	0.769
147A	430	160	4470.5	3.920	0.877	
B	430	160	4495 8	3.572	0.795	

(Continued next page)

TABLE 3 (Continued)

WEIGHT OF THE ALUMINUM-RICH ALLOY LAYER ON ZINC COATINGS CONTAINING ABOUT 0.20 PER CENT ALUMINUM WITH 0.002 TO 0.007 PER CENT IRON DETERMINED BY THE SULFURIC ACID-SODIUM HYDROXIDE WEIGH-STRIP-WEIGH METHOD

Sample Number	Temperature °C	Immersion Time Seconds	Area (Both Sides) sq. mm.	Weight of Alloy Layer mg.	Weight g./sq. m.	Average g./sq. m.
148A	430	320	4506.0	4.416	0.980	
B	430	320	4506.0	4.420	0.981	0.956
149A	430	320	4470.5	4.101	0.917	
B	430	320	4488.2	4.235	0.944	
120A	450	20	4498.3	2.486	0.553	
B	450	20	4523.7	2.495	0.552	0.535
121A	450	20	4533.9	2.344	0.517	
B	450	20	4493.3	2.330	0.519	
122A	450	40	4493.3	2.638	0.587	
B	450	40	4493.3	2.556	0.569	0.557
123A	450	40	4470.5	2.479	0.555	
B	450	40	4539.0	2.343	0.516	
124A	450	80	4546.6	2.850	0.627	
B	450	80	4488.2	2.753	0.613	0.610
125A	450	80	4511.0	2.751	0.610	
B	450	80	4498.3	2.659	0.591	

(Continued next page)

TABLE 3 (Continued)

WEIGHT OF THE ALUMINUM-RICH ALLOY LAYER ON ZINC COATINGS CONTAINING ABOUT 0.20 PER CENT ALUMINUM WITH 0.002 TO 0.007 PER CENT IRON DETERMINED BY THE SULFURIC ACID-SODIUM HYDROXIDE WEIGH-STRIP-WEIGH METHOD

Sample Number	Temperature °C	Immersion Time Seconds	Area (Both Sides) sq. mm.	Weight of Alloy Layer mg.	Weight g./sq. m.	Average g./sq. m.
126A	450	160	4506.0	3.036	0.674	
B	450	160	4493.3	3.030	0.674	0.690
127A	450	160	4541.4	3.277	0.722	
B	450	160	4533.9	3.120	0.688	
128A	450	320	4523.7	4.031	0.891	
B	450	320	4564.3	3.904	0.855	0.942
129A	450	320	4569.5	4.762	1.042	
B	450	320	4546.6	4.450	0.979	
100A	470	20	4483.2	2.890	0.645	
B	470	20	4485.6	2.860	0.638	0.633
101A	470	20	4488.2	2.792	0.622	
B	470	20	4447.7	2.790	0.627	
102A	470	40	4488.2	3.226	0.719	
B	470	40	4493.3	3.314	0.738	0.720
103A	470	40	4533.9	3.271	0.721	
B	470	40	4523.7	3.175	0.702	

(Continued next page)

TABLE 3 (Continued)

WEIGHT OF THE ALUMINUM-RICH ALLOY LAYER ON ZINC COATINGS CONTAINING ABOUT 0.20 PER CENT ALUMINUM WITH 0.002 to 0.007 PER CENT IRON DETERMINED BY THE SULFURIC ACID-SODIUM HYDROXIDE WEIGH-STRIP-WEIGH METHOD

Sample Number	Temperature °C	Immersion Time Seconds	Area (Both Sides) sq. mm.	Weight of Alloy Layer mg.	Weight g./sq. m.	Average g./sq. m.
104A	470	80	4465.4	4.130	0.925	
B	470	80	4506.0	3.947	0.876	0.865
105A	470	80	4523.7	3.730	0.825	
B	470	80	4523.7	3.770	0.833	
106A	470	160	4533.9	5.263	1.161	
B	470	160	4475.5	5.358	1.197	1.145
107A	470	160	4506.0	4.941	1.097	
B	470	160	4488.2	5.047	1.124	
108A	470	320	4531.2	6.957	1.535	
B	470	320	4541.4	7.758	1.708	1.628
109A	470	320	4541.4	7.251	1.597	
B	470	320	4488.2	7.502	1.671	

TABLE 4

WEIGHT OF THE ALUMINUM-RICH ALLOY LAYER ON ZINC COATINGS CONTAINING ABOUT 0.20 PER CENT ALUMINUM WITH 0.011 TO 0.015 PER CENT IRON DETERMINED BY THE SULFURIC ACID-SODIUM HYDROXIDE WEIGH-STRIP-WEIGH METHOD

Sample Number	Temperature °C	Immersion Time Seconds	Area (Both Sides) sq. mm.	Weight of Alloy Layer mg.	Weight g./sq. m.	Average g./sq. m.
150A	430	20	4523.7	2.429	0.537	
B	430	20	4498.3	2.404	0.534	
151A	430	20	4549.2	2.771	0.609	0.573
B	430	20	4488.2	2.749	0.612	
152A	430	40	4488.2	3.302	0.736	
B	430	40	4488.2	3.347	0.746	
153A	430	40	4521.2	3.420	0.756	0.740
B	430	40	4528.8	3.275	0.723	
154A	430	80	4541.4	3.137	0.691	
B	430	80	4516.1	2.957	0.655	
155A	430	80	4546.6	3.644	0.801	0.750
B	430	80	4539.0	3.877	0.854	
156A	430	160	4528.8	5.347	1.181	
B	430	160	4470.5	5.037	1.127	
157A	430	160	4528.8	5.353	1.182	1.169
B	430	160	4516.1	5.349	1.184	

(Continued next page)

TABLE 4 (Continued)

WEIGHT OF THE ALUMINUM-RICH ALLOY LAYER ON ZINC COATINGS CONTAINING ABOUT 0.20 PER CENT ALUMINUM WITH 0.011 TO 0.015 PER CENT IRON DETERMINED BY THE SULFURIC ACID-SODIUM HYDROXIDE WEIGH-STRIP-WEIGH METHOD

Sample Number	Temperature °C	Immersion Time Seconds	Area (Both Sides) sq. mm.	Weight of Alloy Layer mg.	Weight g./sq. m.	Average g./sq. m.
158A	430	320	4483.2	5.610	1.251	
B	430	320	4516.1	5.720	1.267	
159A	430	320	4536.3	7.686	1.694	1.374
B	430	320	4470.5	5.734	1.283	
130A	450	20	4551.7	2.504	0.550	
B	450	20	4498.3	2.427	0.540	
131A	450	20	4541.4	2.442	0.538	0.540
B	450	20	4541.4	2.410	0.531	
132A	450	40	4503.4	2.645	0.587	
B	450	40	4551.7	2.720	0.598	
133A	450	40	4556.8	2.734	0.600	0.591
B	450	40	4582.1	2.644	0.577	

(Continued next page)

TABLE 4 (Continued)

WEIGHT OF THE ALUMINUM-RICH ALLOY LAYER ON ZINC COATINGS CONTAINING ABOUT 0.20 PER CENT ALUMINUM WITH 0.011 TO 0.015 PER CENT IRON DETERMINED BY THE SULFURIC ACID-SODIUM HYDROXIDE WEIGH-STRIP-WEIGH METHOD

Sample Number	Temperature °C	Immersion Time Seconds	Area (Both Sides) sq. mm.	Weight of Alloy Layer mg.	Weight g./sq. m.	Average g./sq. m.
134A	450	80	4546.6	3.690	0.812	
B	450	80	4569.5	3.550	0.777	0.774
135A	450	80	4551.7	3.508	0.771	
B	450	80	4523.7	3.320	0.734	
136A	450	160	4511.0	4.632	1.027	
B	450	160	4521.2	4.753	1.051	1.022
137A	450	160	4544.1	4.506	0.992	
B	450	160	4526.3	4.609	1.018	
138A	450	320	4569.5	6.905	1.511	
B	450	320	4523.7	6.327	1.399	1.439
139A	450	320	SPECIMEN LOST			
B	450	320	4493.3	6.319	1.406	
110A	470	20	4536.3	3.167	0.698	
B	470	20	4511.0	3.000	0.665	0.697
111A	470	20	4483.2	3.278	0.731	
B	470	20	4523.7	3.140	0.694	

(Continued next page)

TABLE 4 (Continued)

WEIGHT OF THE ALUMINUM-RICH ALLOY LAYER ON ZINC COATINGS CONTAINING ABOUT 0.20 PER CENT ALUMINUM WITH 0.011 TO 0.015 PER CENT IRON DETERMINED BY THE SULFURIC ACID-SODIUM HYDROXIDE WEIGH-STRIP-WEIGH METHOD

Sample Number	Temperature °C	Immersion Time Seconds	Area (Both Sides) sq. mm.	Weight of Alloy Layer mg.	Weight g./sq. m.	Average g./sq. m.
112A	470	40	4528.8	3.773	0.833	
B	470	40	4488.2	4.019	0.895	
113A	470	40	4528.8	4.342	0.959	0.925
B	470	40	4493.3	4.554	1.014	
114A	470	80	4506.0	6.565	1.457	
B	470	80	4511.0	5.964	1.322	
115A	470	80	4506.0	5.777	1.282	1.345
B	470	80	4470.5	5.890	1.318	
116A	470	160	4506.0	8.245	1.830	
B	470	160	4470.5	8.330	1.863	
117A	470	160	4523.7	8.548	1.890	1.891
B	470	160	4460.4	8.842	1.982	
118A	470	320	4488.2	15.398	3.431	
B	470	320	4493.3	16.025	3.566	
119A	470	320	4500.9	17.003	3.778	3.607
B	470	320	4457.8	16.277	3.651	

TABLE 5

WEIGHT OF THE ALUMINUM-RICH ALLOY LAYER ON ZINC COATINGS CONTAINING ABOUT 0.30 PER CENT ALUMINUM WITH 0.004 TO 0.006 PER CENT IRON DETERMINED BY THE SULFURIC ACID-SODIUM HYDROXIDE WEIGH-STRIP-WEIGH METHOD

Sample Number	Temperature °C	Immersion Time Seconds	Area (Both Sides) sq. mm.	Weight of Alloy Layer mg.	Weight g./sq. m.	Average g./sq. m.
20A	430	20	4654.0	2.6	0.560	
20B	430	20	4450.0	2.8	0.630	
20C	430	20	4521.2	2.290	0.507	
20D	430	20	4521.2	2.602	0.575	0.601
4A-1	430	20	4493.3	3.036	0.677	
4A-2	430	20	4513.5	2.951	0.654	
40A	430	40	4654.0	3.8	0.817	
40B	430	40	4698.8	3.3	0.703	
40C	430	40	4457.1	2.710	0.608	
40D	430	40	3871.0	2.570	0.664	0.642
8A-1	430	40	4493.3	2.375	0.530	
8A-2	430	40	4513.5	2.380	0.527	
80A	430	80	4609.3	3.6	0.781	
80B	430	80	4583.5	3.4	0.742	
80C	430	80	3225.8	2.580	0.800	
80D	430	80	3505.2	2.930	0.836	0.736
12A-1	430	80	4488.2	2.950	0.657	
12A-2	430	80	4503.4	2.687	0.597	

(Continued next page)

TABLE 5 (Continued)

WEIGHT OF THE ALUMINUM-RICH ALLOY LAYER ON ZINC COATINGS CONTAINING ABOUT 0.30 PER CENT ALUMINUM WITH 0.004 TO 0.006 PER CENT IRON DETERMINED BY THE SULFURIC ACID-SODIUM HYDROXIDE WEIGH-STRIP-WEIGH METHOD

Sample Number	Temperature °C	Immersion Time Seconds	Area (Both Sides) sq. mm.	Weight of Alloy Layer mg.	Weight g./sq. m.	Average g./sq. m.
160A	430	160	4272.0	4.8	1.124	
160B	430	160	4609.3	4.4	0.955	
160C	430	160	4521.2	3.500	0.744	
160D	430	160	3175.0	2.727	0.860	0.862
16A-1	430	160	4516.1	3.537	0.784	
16A-2	430	160	4508.5	3.031	0.672	
320A	430	320	4615.0	4.4	0.954	
320B	430	320	4609.3	4.2	0.911	
320C	430	320	3556.0	3.519	0.990	
320D	430	320	4069.1	4.136	1.017	0.905
20A-1	430	320	4498.3	3.498	0.778	
20A-2	430	320	4513.5	3.520	0.780	
20E	450	20	4385.5	1.9	0.433	
20F	450	20	4564.5	1.7	0.373	
20G	450	20	4440.0	1.841	0.414	
20H	450	20	4521.2	1.555	0.345	0.380
24A-1	450	20	4493.3	1.559	0.347	
24A-2	450	20	4503.4	1.614	0.358	

(Continued next page)

TABLE 5 (Continued)

WEIGHT OF THE ALUMINUM-RICH ALLOY LAYER ON ZINC COATINGS CONTAINING ABOUT 0.30 PER CENT ALUMINUM WITH 0.004 TO 0.006 PER CENT IRON DETERMINED BY THE SULFURIC ACID-SODIUM HYDROXIDE WEIGH-STRIP-WEIGH METHOD

Sample Number	Temperature °C	Immersion Time Seconds	Area (Both Sides) sq. mm.	Weight of Alloy Layer mg.	Weight g./sq. m.	Average g./sq. m.
40E	450	40	4475.0	2.5	0.559	
40F	450	40	4519.8	1.9	0.420	
40G	450	40	4485.6	2.222	0.495	
40H	450	40	4485.6	2.049	0.457	0.441
28A-1	450	40	4541.5	1.635	0.361	
28A-2	450	40	4538.8	1.588	0.350	
80E	450	80	4405.5	2.3	0.522	
80F	450	80	4475.0	2.0	0.447	
80G	450	80	4541.5	1.917	0.423	
80H	450	80	4521.2	1.894	0.418	0.442
32A-1	450	80	4533.9	1.868	0.412	
32A-2	450	80	4503.4	1.931	0.429	
160E	450	160	4609.3	2.4	0.521	
160F	450	160	4609.3	2.3	0.499	
160G	450	160	4064.0	1.769	0.436	
160H	450	160	4521.2	2.026	0.449	0.453
36A-1	450	160	4533.9	1.943	0.428	
36A-2	450	160	4518.6	1.746	0.387	

(Continued next page)

TABLE 5 (Continued)

WEIGHT OF THE ALUMINUM-RICH ALLOY LAYER ON ZINC COATINGS CONTAINING ABOUT 0.30 PER CENT ALUMINUM WITH 0.004 TO 0.006 PER CENT IRON DETERMINED BY THE SULFURIC ACID-SODIUM HYDROXIDE WEIGH-STRIP-WEIGH METHOD

Sample Number	Temperature °C	Immersion Time Seconds	Area (Both Sides) sq. mm.	Weight of Alloy Layer mg.	Weight g./sq. m.	Average g./sq. m.
320E	450	320	4583.5	2.7	0.589	
320F	450	320	4583.5	3.2	0.698	
320G	450	320	3376.8	1.835	0.545	
320H	450	320	4485.6	2.694	0.600	0.564
40A-1	450	320	4523.7	2.120	0.469	
40A-2	450	320	4521.2	2.245	0.498	
20I	470	20	4405.5	2.0	0.454	
20J	470	20	4583.5	2.5	0.545	
20K	470	20	4531.4	2.668	0.589	
20L	470	20	4521.2	2.651	0.586	0.495
44A-1	470	20	4478.1	1.825	0.409	
44A-2	470	20	4503.4	1.723	0.382	
40I	470	40	4539.0	2.4	0.530	
40J	470	40	4698.8	2.2	0.468	
40K	470	40	4475.5	2.952	0.659	
40L	470	40	4531.4	2.826	0.625	0.532
48A-1	470	40	4541.4	2.041	0.449	
48A-2	470	40	4526.3	2.078	0.460	

(Continued next page)

TABLE 5 (Continued)

WEIGHT OF THE ALUMINUM-RICH ALLOY LAYER ON ZINC COATINGS CONTAINING ABOUT 0.30 PER CENT ALUMINUM WITH 0.004 TO 0.006 PER CENT IRON DETERMINED BY THE SULFURIC ACID-SODIUM HYDROXIDE WEIGH-STRIP-WEIGH METHOD

Sample Number	Temperature °C	Immersion Time Seconds	Area (Both Sides) sq. mm.	Weight of Alloy Layer mg.	Weight g./sq. m.	Average g./sq. m.
80I	470	80	4583.5	2.7	0.590	
80J	470	80	4583.5	2.5	0.545	
80K	470	80	4495.7	2.725	0.607	
80L	470	80	4495.7	2.716	0.605	0.541
52A-1	470	80	4465.4	2.034	0.455	
52A-2	470	80	4498.3	1.991	0.442	
160I	470	160	4539.0	4.1	0.903	
160J	470	160	4539.0	4.2	0.925	
160K	470	160	4475.5	3.273	0.731	
160L	470	160	4531.4	3.439	0.759	0.709
56A-1	470	160	4465.4	1.980	0.443	
56A-2	470	160	4498.3	2.224	0.494	
320I	470	320	4583.5	4.9	1.070	
320J	470	320	4564.5	4.6	1.010	
320K	470	320	4521.2	4.679	1.035	
320L	470	320	4475.5	4.671	1.043	0.900
60A-1	470	320	4503.4	2.859	0.635	
60A-2	470	320	4483.2	2.716	0.607	

TABLE 6

AVERAGE WEIGHT OF THE ALUMINUM-RICH ALLOY LAYER ON ZINC COATINGS CONTAINING ABOUT 0.20 AND 0.30 PER CENT ALUMINUM WITH LOW AND INTERMEDIATE IRON LEVELS

Temperature °C	Immersion Time Seconds	Weight of Alloy Layer 0.20% Al 0.002 to 0.007% Fe	Weight of Alloy Layer 0.20% Al 0.011 to 0.015% Fe	Weight of Alloy Layer 0.30% Al 0.004 to 0.006% Fe
430	20	0.771 g./sq. m.	0.573 g./sq. m.	0.601 g./sq. m.
	40	0.731	0.740	0.642
	80	0.811	0.750	0.736
	160	0.769	1.169	0.862
	320	0.956	1.374	0.905
450	20	0.535	0.540	0.380
	40	0.557	0.591	0.441
	80	0.610	0.774	0.442
	160	0.690	1.022	0.453
	320	0.942	1.439	0.564
470	20	0.633	0.697	0.495
	40	0.720	0.925	0.532
	80	0.865	1.345	0.541
	160	1.145	1.891	0.709
	320	1.628	3.607	0.900

Finally, the weight of alloy data shown in Tables 3, 4, and 5 were analyzed statistically by an analysis of variance. The significance of time, temperature and iron content were above the 99 per cent confidence level for each bath composition. Thus, the differences among variables shown in these data are statistically significant.

X-Ray Diffraction Data

X-ray diffraction analysis results for the alloy layers on zinc overlay stripped coatings are shown in Tables 7, 8 and 9. Only coatings made for the shortest and longest immersion time at each bath temperature were analyzed.

Table 10 shows the d-spacings and intensities of the diffraction lines for Fe_2Al_5 as reported in the ASTM X-ray Data File and as reported by Frame[22] in an unpublished thesis. Frame's X-ray data were obtained for Fe_2Al_5 using chromium radiation and a vanadium filter, the same as that used in this work. The ASTM data were obtained using molybdenum radiation.

The d-spacings obtained for the alloy layers on these coatings are in good agreement with those reported for Fe_2Al_5. However, the relative intensities of the diffraction lines vary from the standard data. In general, intensities are greater than those reported.

Based on these data, the evidence indicates that the alloy layer on these coatings is essentially Fe_2Al_5. However, the greater intensities, the slightly displaced d-spacings and the presence of additional lines

TABLE 7

SURFACE X-RAY DIFFRACTION RESULTS FOR THE ALLOY LAYER ON COATINGS CONTAINING ABOUT 0.20 PER CENT ALUMINUM WITH 0.002 TO 0.007 PER CENT IRON

430 °C				450 °C				470 °C				Identification	
20 Sec. Immersion		320 Sec. Immersion		20 Sec. Immersion		320 Sec. Immersion		20 Sec. Immersion		320 Sec. Immersion			
d*	Int**	d*	Int**	d*	Int**	d*	Int**	d*	Int**	d*	Int**	Phase	hkl
4.96	30	4.96	20	4.94	44	4.94	23	4.92	25	4.98	12	Fe_2Al_5	110
3.84	46	3.85	52	3.82	50	3.82	28	3.83	32	3.84	45	Fe_2Al_5	200
3.22	60	3.23	70	3.20	94	3.21	46	3.22	48	3.22	40	Fe_2Al_5	111
		2.38	21			2.36	13	2.37	16	2.37	9	Fe_2Al_5	220
2.12	76	2.13	100	2.12	73	2.13	79	2.13	80	2.13	97	Fe_2Al_5	030, 002
2.07	100	2.07	90	2.05	100	2.06	100	2.07	100	2.07	100	Fe_2Al_5	311
1.95	15	1.95	31			1.95	14	1.95	16	1.95	19	Fe_2Al_5	112
		1.91	15							1.91	11	Fe_2Al_5	400
		1.77	21							1.77	11	Fe_2Al_5	022
1.58	30	1.58	31	1.57	67	1.57	29	1.58	32	1.59	14	Fe_2Al_5	040
										1.53	6	Fe_2Al_5	500
										1.48	14	Fe_2Al_5	501
										1.27	6	Fe_2Al_5	023
				1.23	58	1.24	15	1.24	16	1.24	24	Fe_2Al_5	530
										1.22	12	--	--
										1.21	19	Fe_2Al_5	313

* d-Spacing
** Intensity

TABLE 8

SURFACE X-RAY DIFFRACTION RESULTS FOR THE ALLOY LAYER ON COATINGS CONTAINING ABOUT 0.20 PER CENT ALUMINUM WITH 0.011 TO 0.015 PER CENT IRON

430 °C				450 °C				470 °C				Identification	
20 Sec. Immersion		320 Sec. Immersion		20 Sec. Immersion		320 Sec. Immersion		20 Sec. Immersion		320 Sec. Immersion			
d*	Int**	d*	Int**	d*	Int**	d*	Int**	d*	Int**	d*	Int**	Phase	hkl
4.94	43	4.94	24	4.94	29	4.94	13	4.94	21	4.96	5	Fe_2Al_5	110
3.84	36	3.84	51	3.84	29	3.83	43	3.83	31	3.82	46	Fe_2Al_5	200
3.21	88	3.22	80	3.22	100	3.22	50	3.21	47	3.22	45	Fe_2Al_5	111
		3.02	12	3.02	17	3.02	7					--	--
										2.72	9	--	--
		2.57	15	2.57	21							--	--
										2.47	4	--	--
										2.42	5	--	--
						2.37	11			2.37	13	Fe_2Al_5	220
2.12	100	2.12	68	2.13	100	2.13	100	2.13	87	2.13	65	Fe_2Al_5	030, 002
										2.12	26	--	--
2.07	63	2.07	100	2.07	71	2.07	73	2.07	100	2.07	100	Fe_2Al_5	311
		1.95	29			1.95	13	1.95	7	1.95	14	Fe_2Al_5	112

* d-Spacing
** Intensity

(Continued next page)

TABLE 8 (Continued)

SURFACE X-RAY DIFFRACTION RESULTS FOR THE ALLOY LAYER ON COATINGS CONTAINING ABOUT 0.20 PER CENT ALUMINUM WITH 0.011 TO 0.015 PER CENT IRON

430 °C				450 °C				470 °C				Identification	
20 Sec. Immersion		320 Sec. Immersion		20 Sec. Immersion		320 Sec. Immersion		20 Sec. Immersion		320 Sec. Immersion			
d*	Int**	d*	Int**	d*	Int**	d*	Int**	d*	Int**	d*	Int**	Phase	hkl
		1.91	12			1.91	9	1.91	21	1.91	11	Fe_2Al_5	400
		1.77	14			1.77	7			1.77	8	Fe_2Al_5	022
										1.64	3	Fe_2Al_5	420
1.59	48	1.58	34	1.58	56	1.57	13			1.62	3	--	--
						1.53	10	1.58	32	1.57	5	Fe_2Al_5	040
										1.53	8	Fe_2Al_5	500
		1.48	21			1.48	8			1.49	3	--	--
										1.48	15	Fe_2Al_5	032
										1.40	7	Fe_2Al_5	501
						1.28	9			1.28	3	Fe_2Al_5	023
										1.25	15	--	--
		1.24	13			1.24	20			1.24	2	Fe_2Al_5	530

* d-Spacing
** Intensity

(Continued next page)

TABLE 8 (Continued)

SURFACE X-RAY DIFFRACTION RESULTS FOR THE ALLOY LAYER ON COATINGS CONTAINING ABOUT 0.20 PER CENT ALUMINUM WITH 0.011 TO 0.015 PER CENT IRON

430 °C				450 °C				470 °C				Identification	
20 Sec. Immersion		320 Sec. Immersion		20 Sec. Immersion		320 Sec. Immersion		20 Sec. Immersion		320 Sec. Immersion			
d*	Int**	d*	Int**	d*	Int**	d*	Int**	d*	Int**	d*	Int**	Phase	hkl
1.23	18			1.23	21					1.23	33	--	--
		1.22	10									--	--
		1.21	20	1.21	30					1.21	18	Fe_2Al_5	313

* d-Spacing
** Intensity

TABLE 9

SURFACE X-RAY DIFFRACTION RESULTS FOR THE ALLOY LAYER ON COATINGS CONTAINING ABOUT 0.30 PER CENT ALUMINUM WITH 0.004 TO 0.006 PER CENT IRON

430 °C				450 °C				470 °C				Identification	
20 Sec. Immersion		320 Sec. Immersion		20 Sec. Immersion		320 Sec. Immersion		20 Sec. Immersion		320 Sec. Immersion			
d*	Int**	d*	Int**	d*	Int**	d*	Int**	d*	Int**	d*	Int**	Phase	hkl
4.96	36	4.93	41	4.91	55	4.94	16	4.94	33	4.94	16	Fe_2Al_5	110
3.85	63	3.82	70	3.83	42	3.83	29	3.83	48	3.83	51	Fe_2Al_5	200
3.21	64	3.22	82	3.20	100	3.22	100	3.22	68	3.22	100	Fe_2Al_5	111
3.02	25	3.02	11	3.02	42							--	--
2.62	36	2.62	13	2.62	36	2.61	13	2.61	21			--	--
		2.57	17	2.57	55	2.57	16					--	--
2.37	25	2.37	23			2.37	8			2.37	14	Fe_2Al_5	220
2.12	100	2.12	66	2.12	82	2.12	48	2.12	77	2.13	99	Fe_2Al_5	030, 020
2.07	32	2.06	100			2.06	38	2.06	100	2.06	100	Fe_2Al_5	311
		1.94	29			1.94	20			1.95	15	Fe_2Al_5	112
1.91	25	1.91	30			1.91	10	1.91	18	1.91	12	Fe_2Al_5	400
1.57	70	1.57	38	1.58	67	1.57	29	1.57	40	1.58	15	Fe_2Al_5	040
		1.53	16							1.54	9	Fe_2Al_5	140

* d-Spacing
** Intensity

(Continued next page)

TABLE 9 (Continued)

SURFACE X-RAY DIFFRACTION RESULTS FOR THE ALLOY LAYER ON COATINGS CONTAINING ABOUT 0.30 PER CENT ALUMINUM WITH 0.004 TO 0.006 PER CENT IRON

430 °C				450 °C				470 °C				Identification	
20 Sec. Immersion		320 Sec. Immersion		20 Sec. Immersion		320 Sec. Immersion		20 Sec. Immersion		320 Sec. Immersion			
d*	Int**	d*	Int**	d*	Int**	d*	Int**	d*	Int**	d*	Int**	Phase	hkl
		1.48	16			1.48	14			1.48	12	Fe_2Al_5	032
		1.40	22									--	--
1.23	21	1.24	16	1.24	42	1.23	11			1.24	15	Fe_2Al_5	530

* d-Spacing
** Intensity

TABLE 10

INTENSITY AND D-SPACING OF DIFFRACTION LINES FOR Fe_2Al_5

MoK Radiation (From ASTM X-Ray Data File)			Cr Radiation and V Filter (From J. W. Frame's Unpublished Thesis)		
d-Spacing	Relative Intensity	hkl	d-Spacing	Relative Intensity	hkl
4.90	11	110			
3.86	24	200	3.86	4	200
3.20	40	111	3.20	46	111
2.39	10	220	2.39	2	220
2.11	100	030,002	2.11	100	030,002
2.05	100	311	2.06	32	311
1.94	10	112	1.94	52	112
1.90	8	400	1.90	--	400
1.84	3	202	1.84	3	202
1.76	8	022	1.76	10	022
1.70	2	122	1.70	2	122
1.63	2	420	1.63	--	420
1.59	2	040	1.59	4	040
1.55	2	140	1.55	4	140
1.52	10	500	1.52	4	500
1.48	16	032	1.48	17	032
1.42	2	501	1.42	4	501
1.39	10	003	1.39	3	003
1.27	10	023	1.27	5	023
1.24	8	530	1.24	4	530
1.21	16	313	1.21	64	313

on some specimens suggest that some other, possibly transition phase which has X-ray characteristics similar to Fe_2Al_5 may also be present. The surfaces analyzed which are similar to those shown on the copper electroplated specimens in Figure 7 indicate that these differences in X-ray data could be associated with the blue-gray particle phase. Moreover, the coatings which show the more pronounced differences in X-ray characteristics from Fe_2Al_5 were made under conditions which seem to favor formation of the blue-gray particles; namely, higher temperatures, longer immersion times, higher iron contents and lower aluminum contents. Thus, the diffraction lines shown are probably for Fe_2Al_5 and the blue-gray particle phase. Furthermore, the lines not assigned to a compound probably are for the blue-gray particle phase.

These X-ray data showed a trend which tends to confirm the weight of alloy data obtained by stripping. Coatings having heavier weights of alloy also showed corresponding more intense diffraction lines, indicating that thicker alloy layers were present.

Electron Microscope Examinations

Again, only coatings made for 20 and 320 seconds at each bath temperature for each bath composition were examined with the electron microscope. This examination revealed that these alloy layers show the following two general types of surfaces.

(1) A relatively smooth surface with some slight relief.

(2) A nodular surface against a granular background.

Some alloy layers, depending upon the coating conditions, also showed surfaces which appeared to be in transition from the smooth to nodular surfaces.

Figure 8 shows coatings with these two general types of alloy surfaces. Notice that the smooth surface is for a coating containing about 0.20 per cent aluminum with 0.002 per cent iron which was made at 430°C for a 20 second immersion and the nodular surface is for a coating containing about 0.20 per cent aluminum with 0.014 per cent iron which was made at 470°C for a 320 second immersion. These general conditions seemed to have favored each particular surface. For example, the higher coating temperatures, longer immersion times and higher iron contents gave alloy layers with nodular surfaces, whereas lower coating temperatures, shorter immersion times and lower iron contents gave alloy layers with smooth surfaces. This suggests that smooth surface alloy layers may form initially under all conditions. However, as temperature and immersion time are increased, the nodules apparently nucleate and grow on this initially smooth surface alloy layer, thereby leading to nodular surface alloy layers. Furthermore, as shown in Figure 9, these nodules apparently can grow into each other to form continuous layers. Thus, these nodules could be a transition phase which may result from a transformation between the bath and the smooth surface alloy layers.

Also notice that conditions favoring nodular growth are the same conditions which tend to favor the formation of the blue-gray particle phase. This is not positive proof but rather a possibility that the

a) 0.22% Al, 0.002% Fe
430°C, 20 second immersion

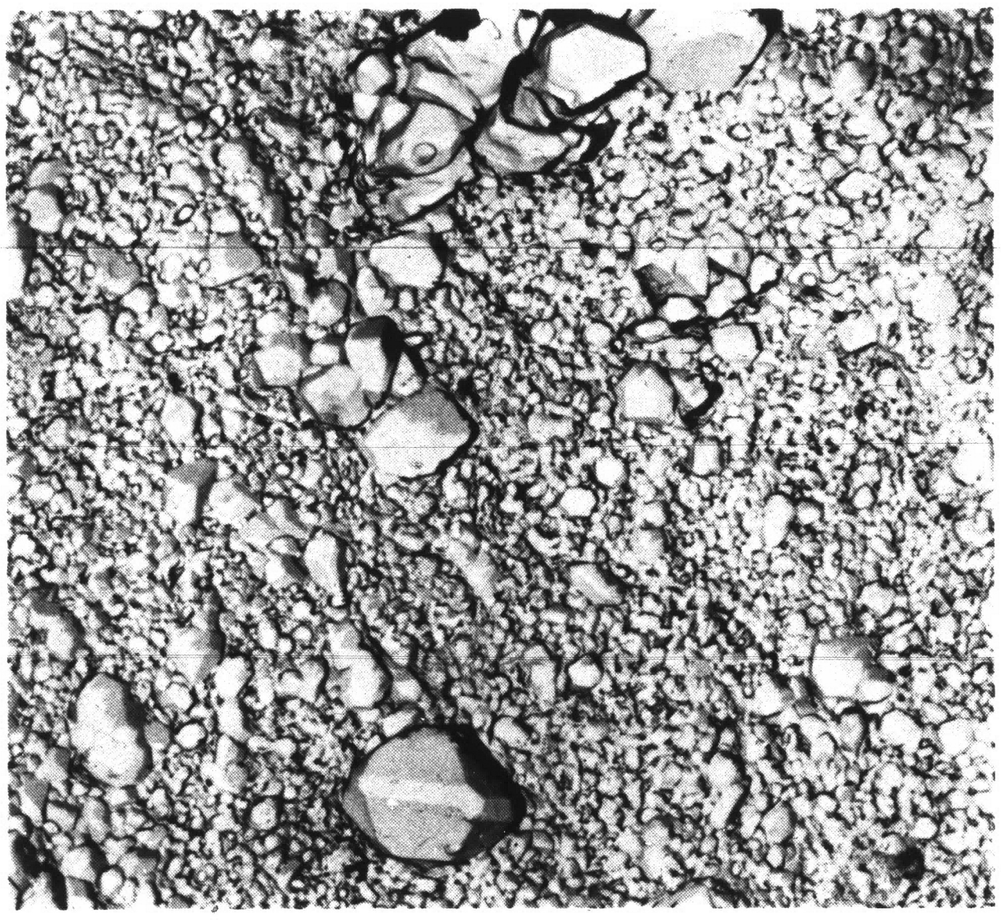

b) 0.20% Al, 0.014% Fe
470°C, 320 second immersion

FIGURE 8. Typical Smooth and Nodular Surfaces Observed on Alloy Layers with the Electron Microscope. 4080X.

FIGURE 9. Agglomerated Growth of Nodules on a Coating Containing 0.21 Per Cent Aluminum with 0.015 Per Cent Iron which was made at 450°C with a 320 Second Immersion. 4080X.

The nodules can grow together to form a continuous layer.

nodules and the blue-gray particles may be the same phase. Conversely, if this is true, then the smooth surfaces may be the Fe_2Al_5 phase.

Careful examination of the nodular surfaces in Figures 8 and 9 indicates that some nodules show a regular crystalline structure. Other similarly shaped nodules were also observed on other specimens during the course of these examinations. Notice particularly the regularly shaped nodule shown in Figure 8b which is shown at an increased magnification of 19,400 X in Figure 10. Members of the Mineralogy Group of the Homer Research Laboratories of Bethlehem Steel Corporation examined the structure of this nodule and indicated that it could be classified as cubic, orthorhombic or tetragonal. More positive techniques for studying crystal structures would have to be used to classify definitely the structure of these nodules.

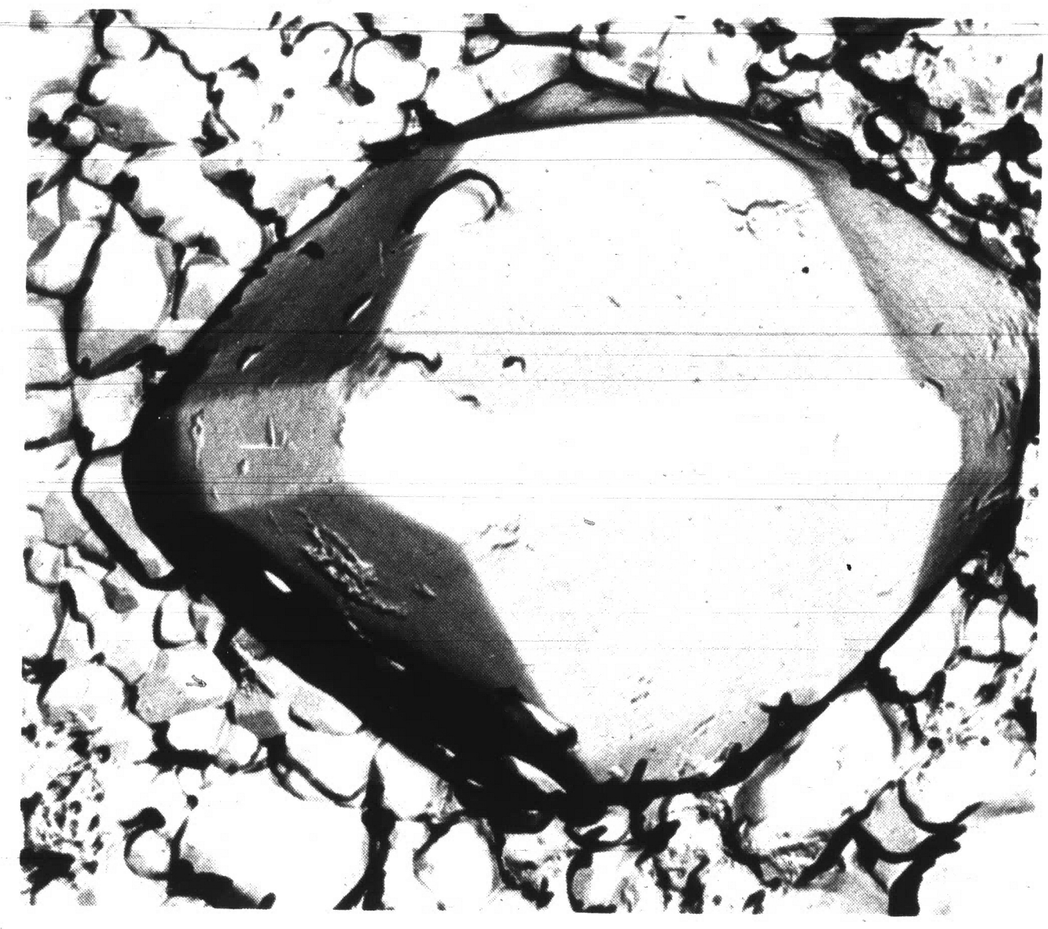

FIGURE 10. High Magnification Crystalline Form of Nodules. 19,400X

The nodule shown is the same as that shown in Figure 8. The structure has been tentatively classified as cubic, orthorhombic or tetragonal.

DISCUSSION OF RESULTS

Growth Rate of the Aluminum-Rich Alloy Layers

The growth rate of alloy layers of iron-zinc and iron-aluminum has been generally established to occur by the parabolic law. An exception to this is the well documented linear rate of growth which occurs with iron-zinc alloy layers in the temperature range of about 480°C to 520°C. Growth of the aluminum-rich alloy layers formed on steel in aluminum-bearing zinc baths in these studies would also be expected to occur parabolically if the growth rate is essentially diffusion controlled. Therefore, a plot of the weight of alloy versus the square root of immersion time should be a straight line.

The additional factor of the availability of aluminum to the growing alloy layer surface must also be considered in the growth of these aluminum-rich alloy layers in aluminum-bearing zinc baths. Unlike alloy layers which grow in straight zinc or straight aluminum baths where an infinite supply of zinc or aluminum atoms is available, these aluminum-rich alloy layers must grow in baths where the availability of aluminum atoms is limited. Thus, local depletion or local unavailability of aluminum to the alloy layer surface probably will affect the growth of the alloy layer. For our purposes, we have assumed that aluminum atoms were generally available because the specimens were agitated during immersion. Therefore, plots of the weight of alloy versus the square root of time were made to characterize the growth of these aluminum-rich alloy layers.

Figures 11, 12 and 13 show the growth of the alloy layer for each bath composition at each of the three bath temperatures. Notice that the plots give reasonably good straight lines between 20 and 320 seconds, indicating that the alloy layer is growing parabolically between these immersion times. An exception to this is the weight of alloy obtained at 320 seconds for the 0.20 per cent aluminum bath with 0.015 per cent iron. This point obviously did not fit the line, for reasons which will be discussed later, and therefore, was not included in the plot.

As shown in Figures 11 and 12, growth of the alloy layer at 430°C and 450°C was similar for each of the baths containing 0.20 per cent aluminum, and, as would be expected, the weight of the alloy layer was heaviest and growth was most rapid at 470°C for both of these baths. However, growth of the alloy layer for the bath containing 0.30 per cent aluminum, shown in Figure 13, was different from that which would be expected. Notice that growth at 430°C was similar to that at 470°C and much greater than that at 450°C. At 430°C the total weight of alloy for 0.30 per cent aluminum was greatest and the rate of growth was about the same as that at 470°C. However, the total weight of alloy was least and growth was apparently slowest at 450°C.

These same data have been replotted for each temperature in Figures 14, 15 and 16 to show the effect of bath composition on the growth of the alloy layer. Also, the growth coefficient in g2/m4/sec. as determined from the slopes of these lines are shown in Table 11.

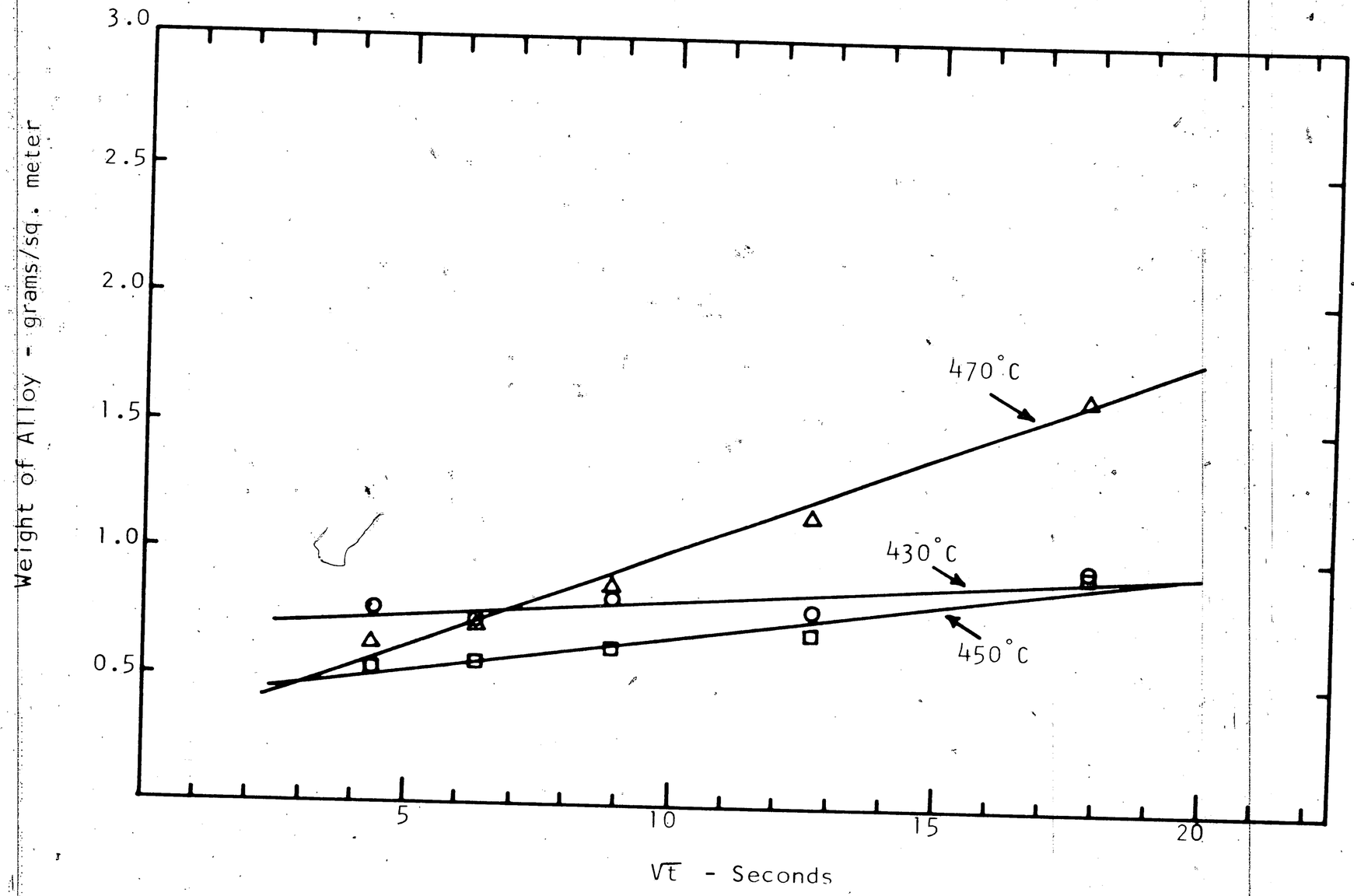

FIGURE 11. Growth of the Alloy Layer for Coatings Containing about 0.20 Per Cent Aluminum with 0.002 to 0.007 Per Cent Iron.

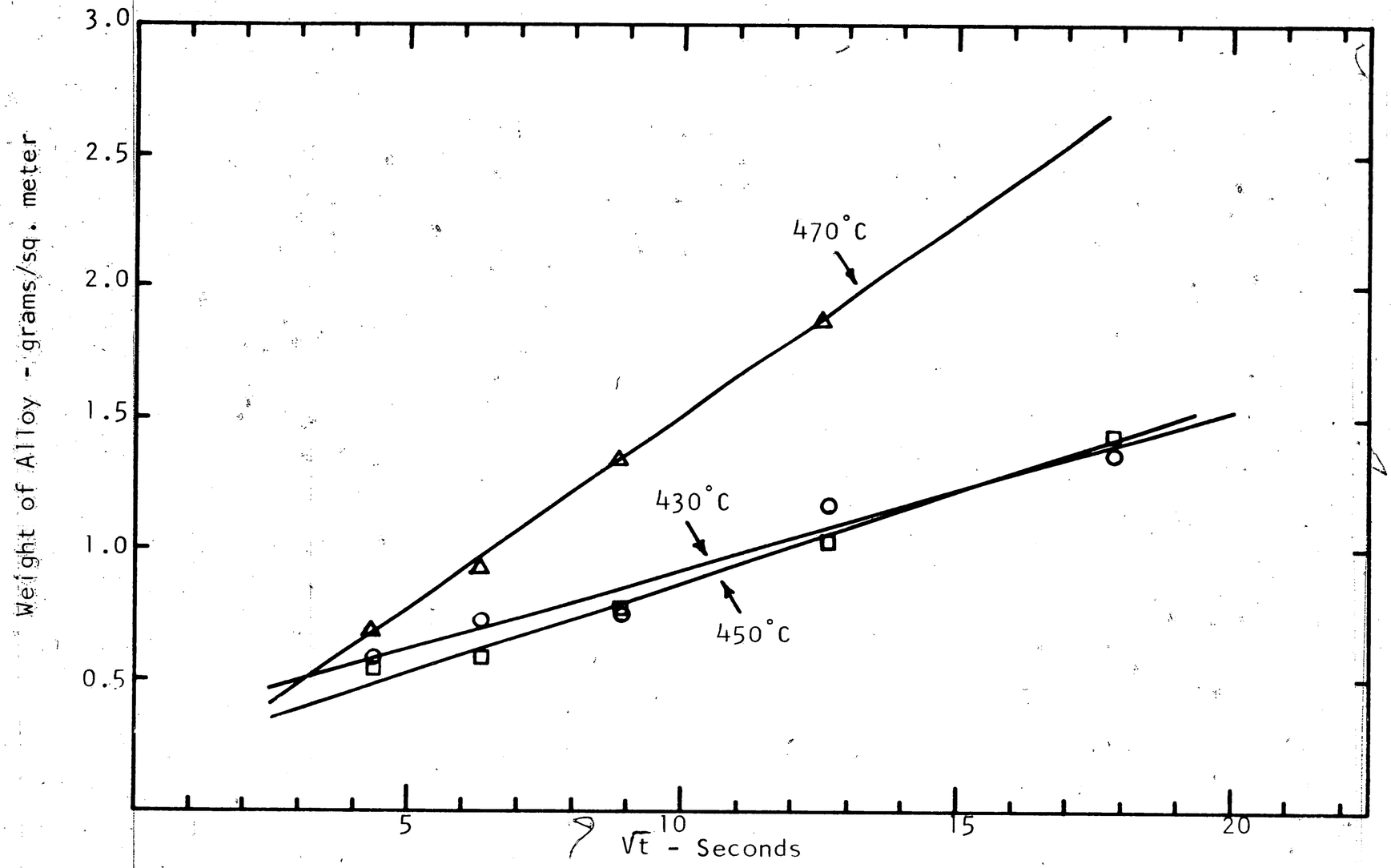

FIGURE 12. Growth of the Alloy Layer for Coatings Containing about 0.20 Per Cent Aluminum with 0.011 to 0.015 Per Cent Iron.

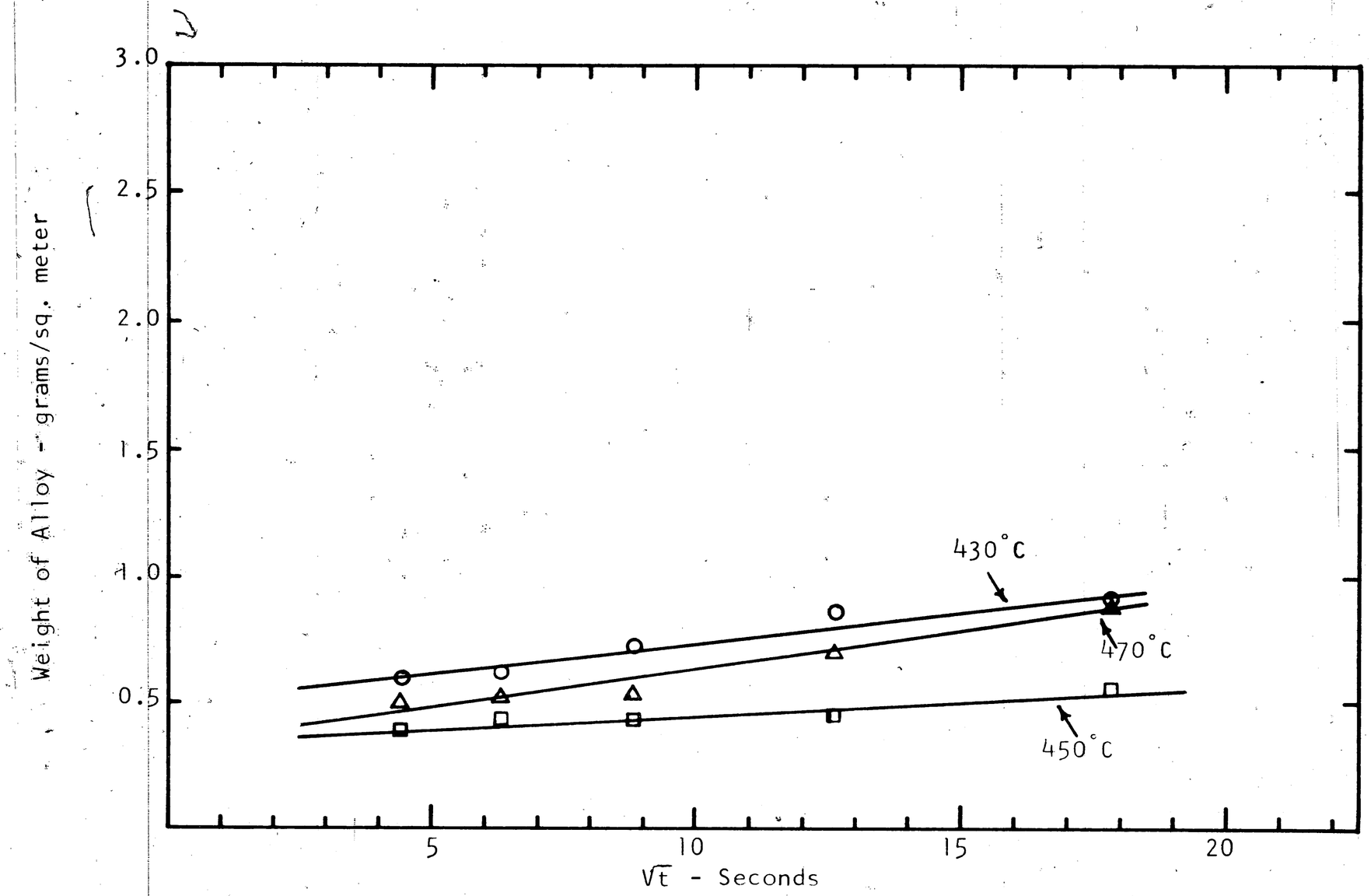

FIGURE 13. Growth of the Alloy Layer for Coatings Containing about 0.30 Per Cent Aluminum with 0.004 to 0.006 Per Cent Iron.

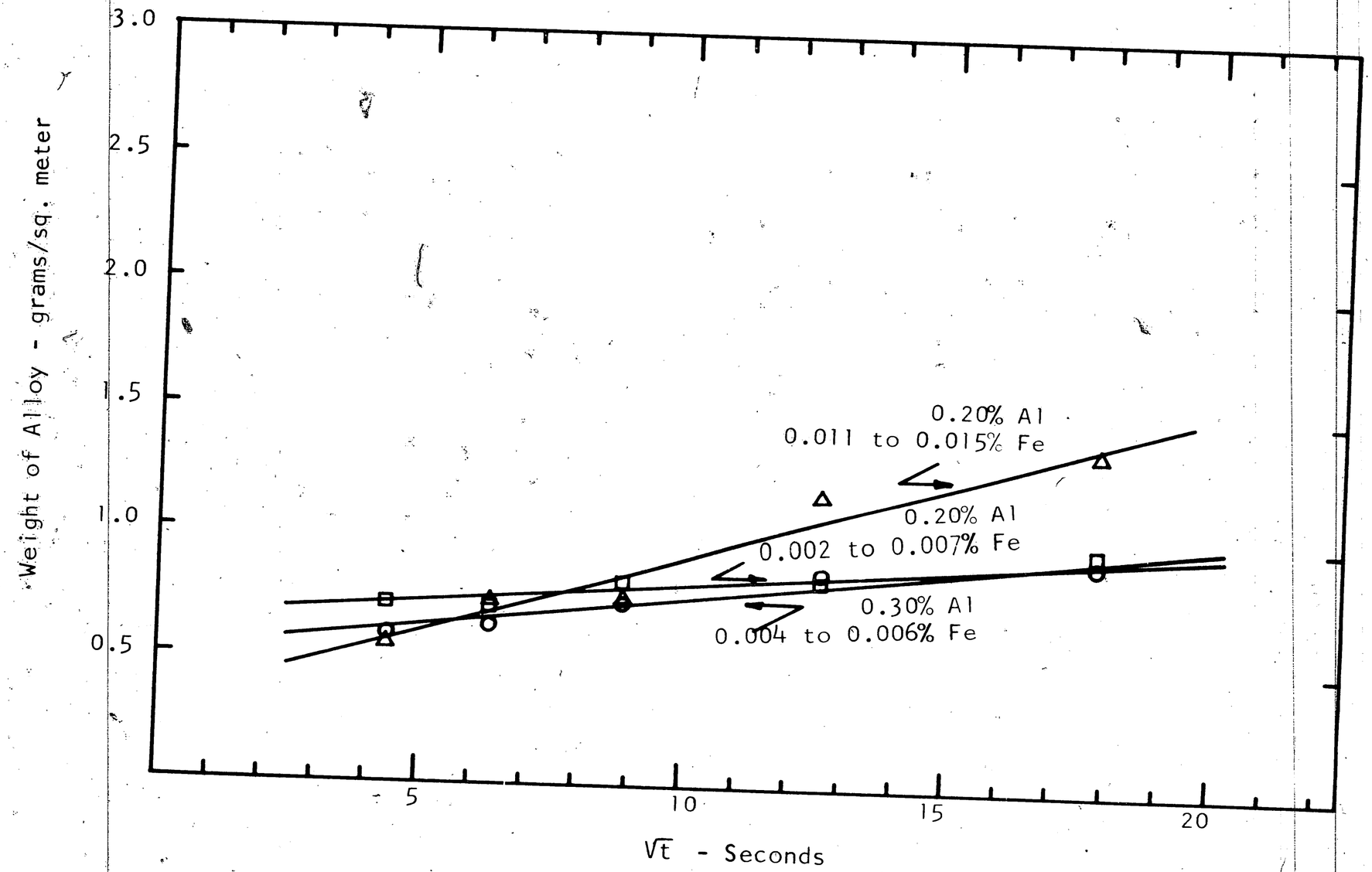

FIGURE 14. Growth of the Alloy Layer for Each Bath Composition at 430°C.

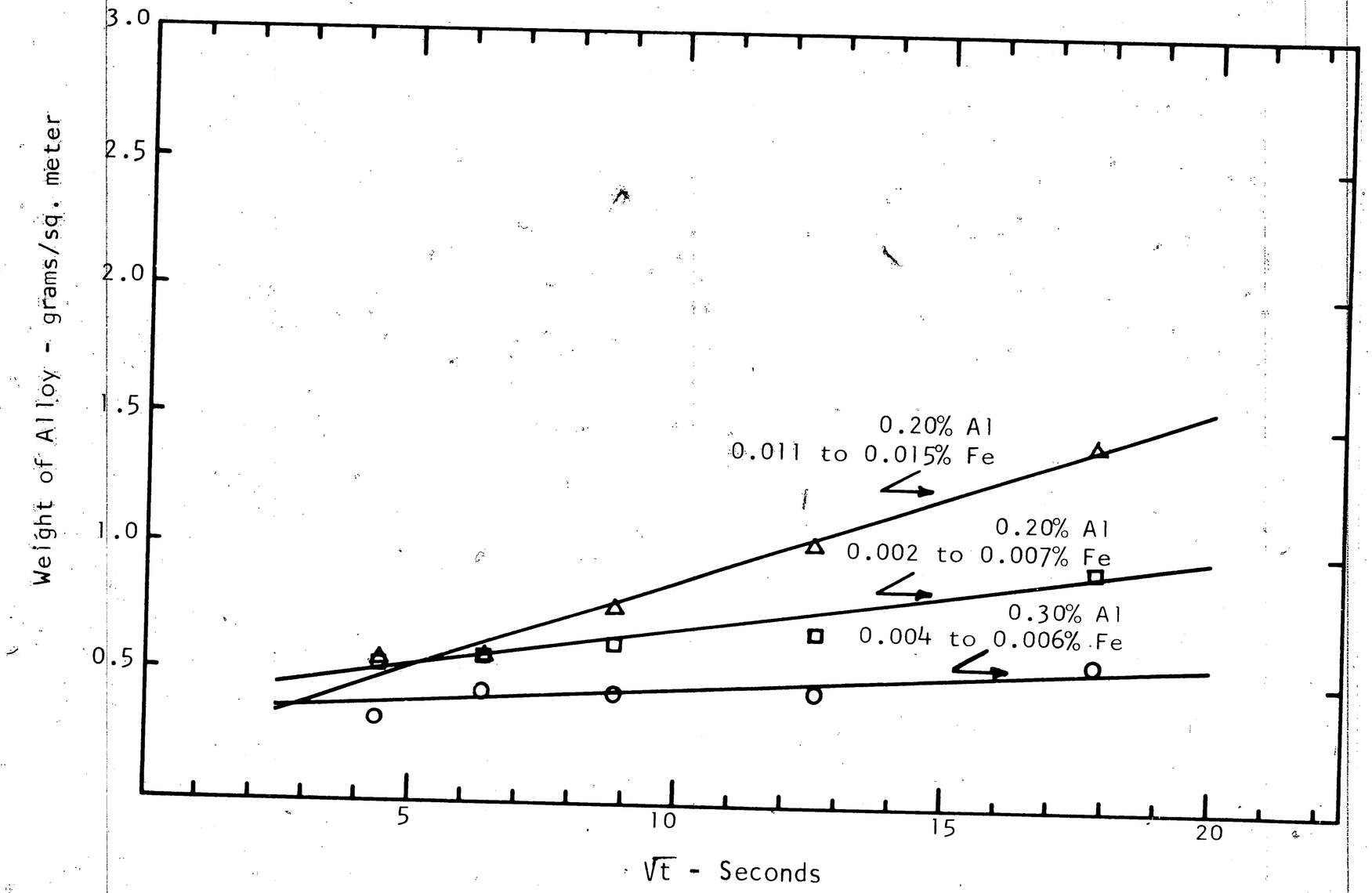

FIGURE 15. Growth of the Alloy Layer for Each Bath Composition at 450°C.

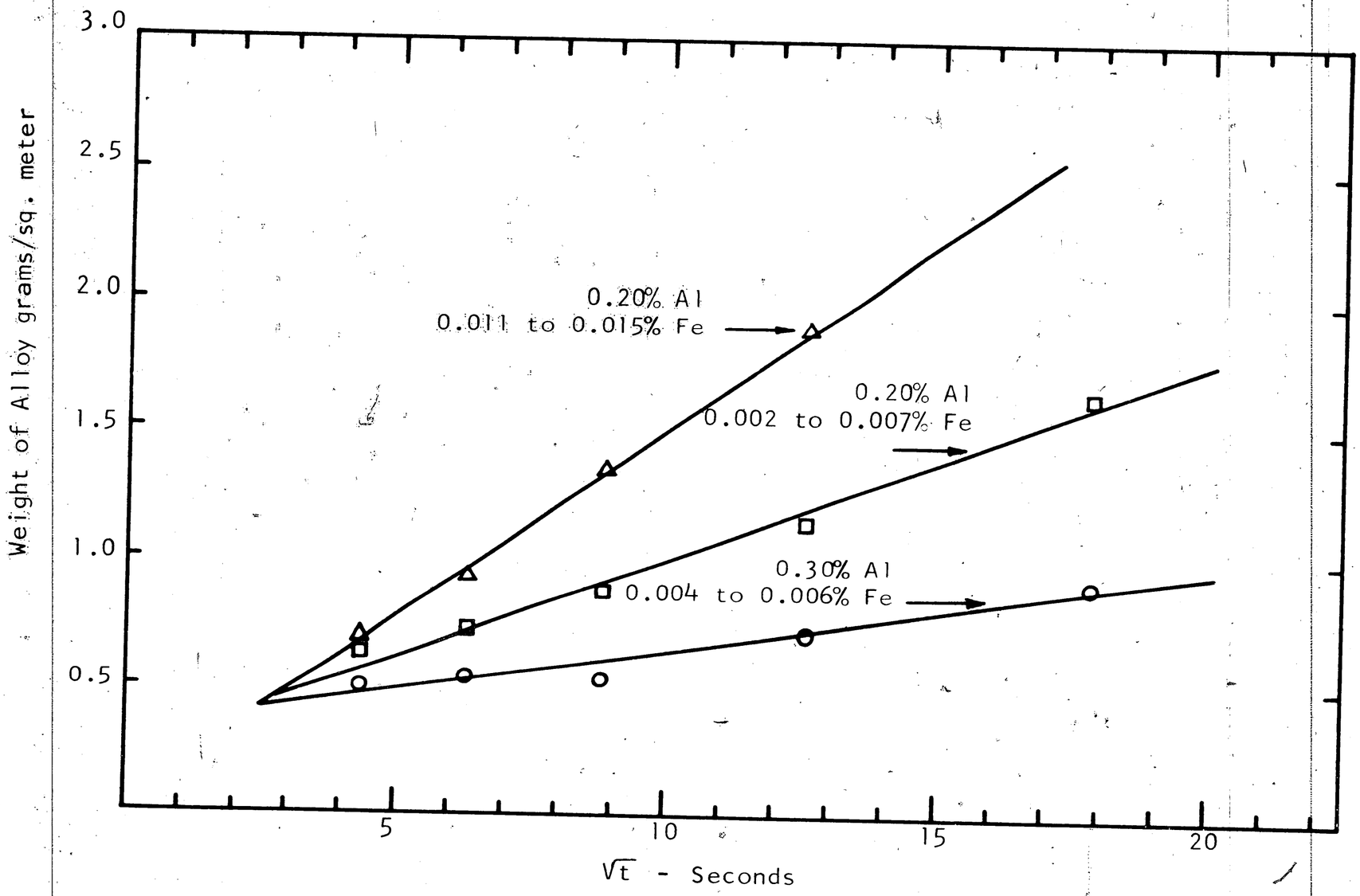

FIGURE 16. Growth of the Alloy Layer for Each Bath Composition at 470°C.

TABLE 11

GROWTH COEFFICIENTS FOR THE ALUMINUM-RICH ALLOY LAYER

$g^2/m^4/sec.$

Bath Temperature	Bath Composition 0.30% Al 0.004 to 0.006% Fe	0.20% Al 0.002 to 0.007% Fe	0.20% Al 0.011 to 0.015% Fe
430°C	6.3×10^{-4}	2.0×10^{-4}	37.2×10^{-4}
450°C	1.2×10^{-4}	8.4×10^{-4}	47.6×10^{-4}
470°C	9.6×10^{-4}	56.3×10^{-4}	216.1×10^{-4}

Coatings with 0.20 per cent aluminum and low iron show generally greater growth than coatings with 0.30 per cent aluminum and low iron, with differences in growth becoming greater as the temperature is increased. Also notice that 0.20 per cent aluminum coatings with high iron show heavier weights of alloy and significantly greater growth rates than 0.20 per cent aluminum coatings with low iron. Again, differences become more pronounced as the temperature is increased. Thus, the aluminum/iron ratio of the bath has a significant effect on the growth of these aluminum-rich alloy layers.

An interesting aspect shown in these plots concerning the effect of iron is the significance of immersion time on the total weight of alloy at a given temperature. Notice that the intersection of the lines for low and intermediate iron levels for 0.20 per cent aluminum occurs at shorter immersion times as the temperature is increased. The intersection of these lines indicates the immersion time at which the weight of the alloy layer is the same for both iron levels. Thus, this indicates that the total weight of alloy will be greater for low iron baths when immersion times are shorter than the intersection time and greater for high iron baths when immersion times are longer than the intersection time.

A plot of this intersection time for baths with 0.002 to 0.005 per cent iron and 0.011 to 0.015 per cent iron at about 0.20 per cent aluminum versus temperature is shown in Figure 17. This plot shows that the

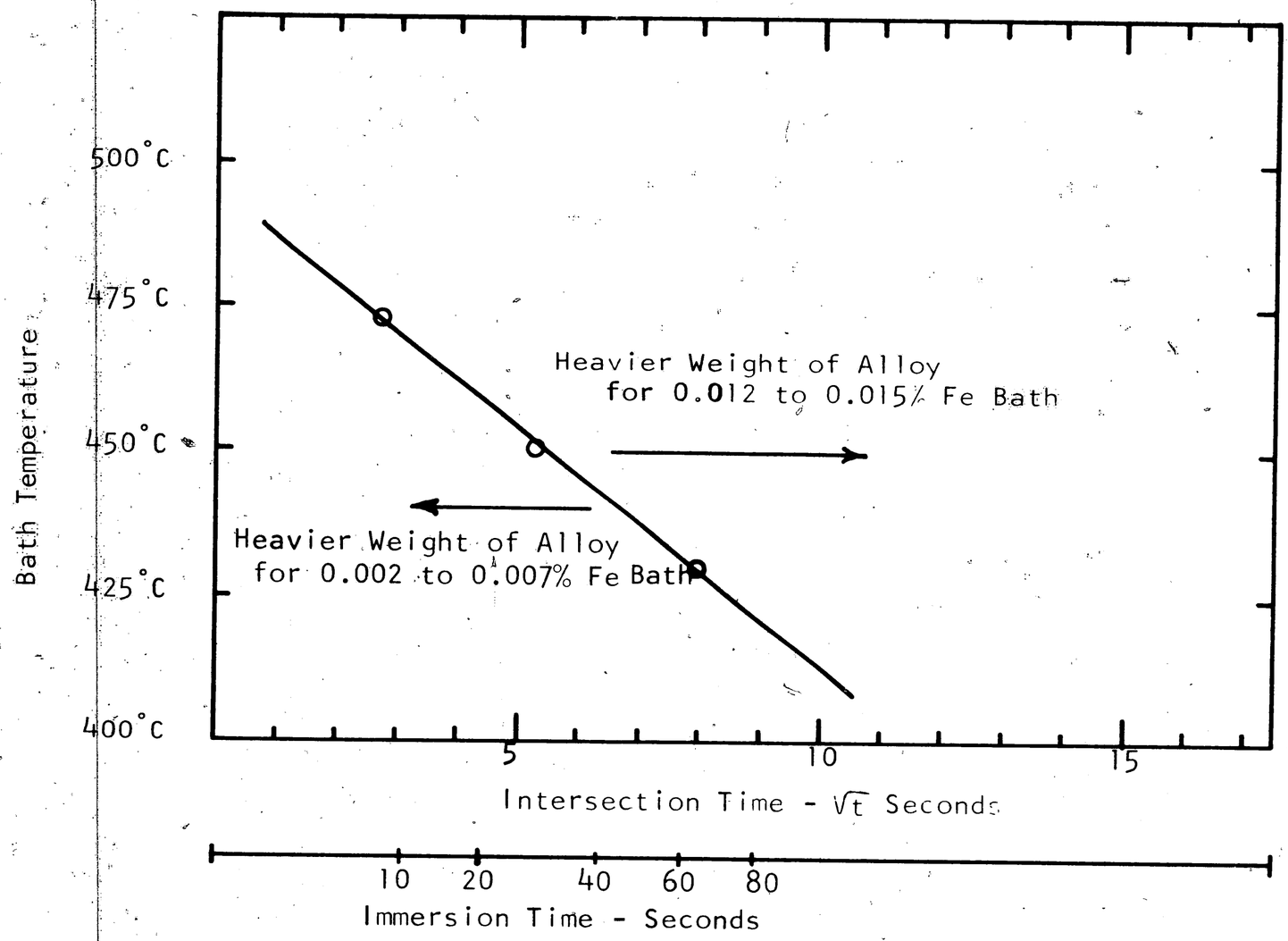

FIGURE 17. Plot of Intersection Time for 0.20 Per Cent Aluminum Coatings with 0.002 to 0.007 Per Cent Iron and 0.012 to 0.015 Per Cent Iron Versus Temperature.

intersection time decreases with increasing temperature, or, at a given temperature, for immersion times less than that indicated by the line, heavier weights of alloy will be obtained for low iron baths and for greater immersion times, heavier weights of alloy will be obtained for high iron baths. Thus, while higher iron content coatings show greater aluminum-rich alloy growth rates than low iron coatings, low iron coatings may show a heavier total weight of alloy, especially for short immersion times.

Duplex Nature of the Aluminum-Rich Alloy Layer

The possible duplex nature of the aluminum-rich alloy layer was indicated by metallographic, X-ray diffraction and electron microscope results. Evidence indicates that the aluminum-rich alloy layer is comprised of a very thin layer, which is not usually resolvable metallographically, and a blue-gray particle phase, which grows as isolated nodules or as occasional bursts. The frequency and size of the blue-gray particle phase was also observed to increase with increasing temperature and immersion time and with the iron content of the bath. Thus, because of this apparently simultaneous growth of two different phases, a kinetic evaluation of the growth of the separate layers comprising the aluminum-rich alloy layer from the growth curves is difficult. However, identification or determination of the composition of the blue-gray particle phase could give insight on the growth rate curves and on the mechanism of inhibition of growth of iron-zinc alloy layers by this aluminum-rich alloy layer.

Accordingly, an electron-probe microanalysis was made of these particles on coatings with the zinc overlay present and on the copper-electroplated coatings with the zinc overlay removed.

Radiation images of localized alloy growths on 0.22 per cent and 0.32 per cent aluminum coatings are shown in Figures 18 and 19. Figure 18 shows radiation images for exactly the same area as that shown for the 0.22 per cent aluminum coating in the photomicrograph in Figure 3b. Blue-gray phase particles are shown adjacent to iron-zinc phases which deeply penetrated the steel where inhibition broke down. Notice that the areas rich in aluminum and iron, and also apparently zinc, are associated with the blue-gray phase particles. Similarly, Figure 19 shows radiation images for bursts of alloy like those shown for the 0.30 per cent aluminum coating in Figure 2. These radiation images again show that iron, zinc and aluminum are apparently concentrated in the alloy bursts. Thus, these results indicate that the blue-gray phase particles are a transition phase containing iron, zinc and aluminum.

There was, however, the possibility in this electron-probe microanalysis that the zinc shown in the particles was associated with the zinc overlay background. Therefore, a similar analysis was made of the blue-gray phase particles on the same 0.22 per cent aluminum coating which was electroplated with copper and which, in turn, eliminated the zinc background. Radiation images and line scans are shown in Figures 20 and 21 for an area which is similar to that shown in the photomicrograph

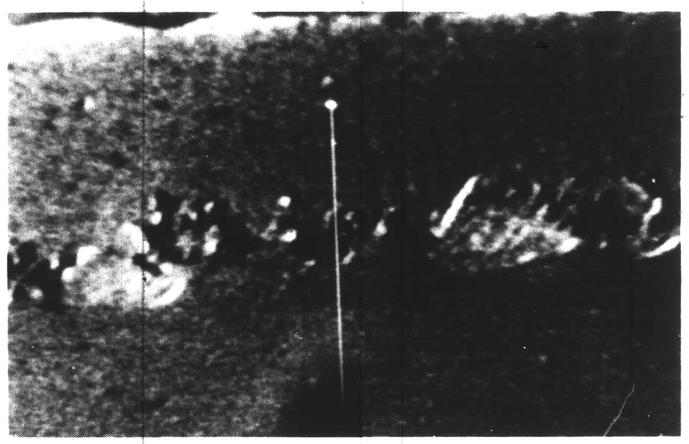

Electron Scanning Image

zinc

steel

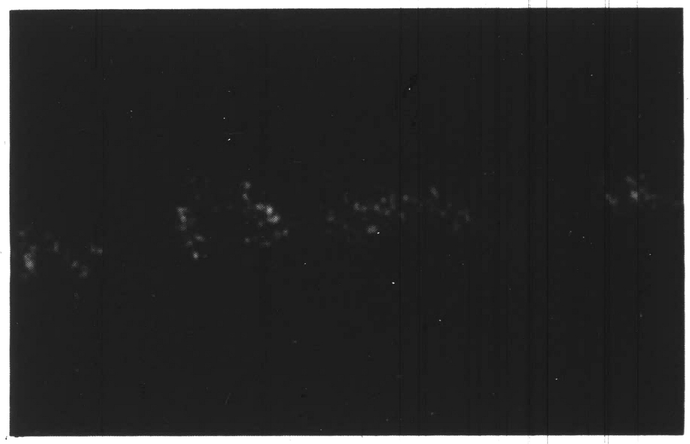

Aluminum Kα Radiation Image

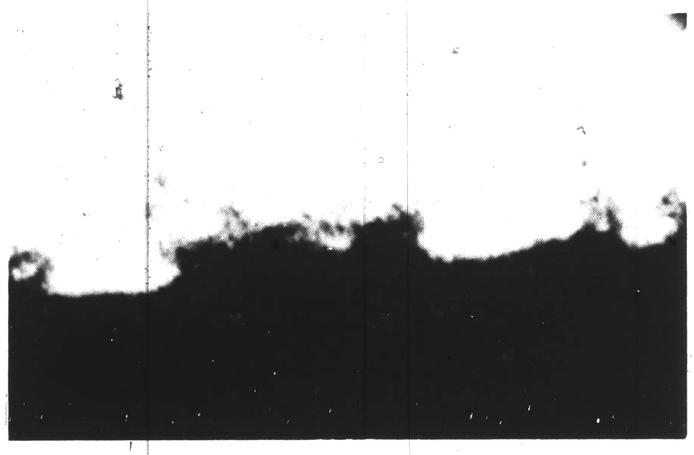

Zinc Kα Radiation Image

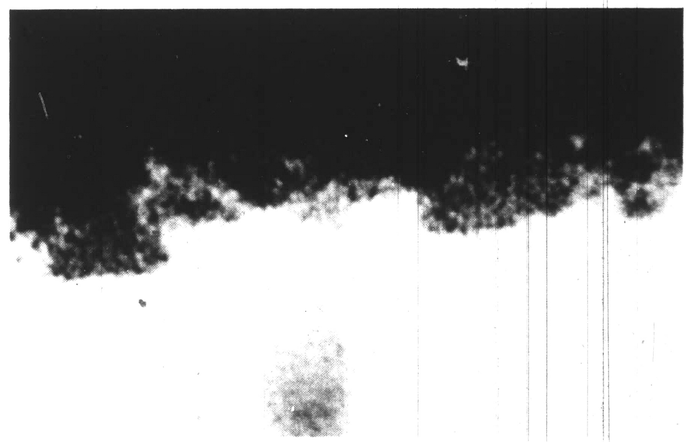

Iron Kα Radiation Image

FIGURE 18. Electron-Probe Microanalysis of Localized Growth on a 0.22 Per Cent Aluminum Coating with 0.014 Per Cent Iron which was made at 470°C with a 320 Second Immersion. 500X

Electron Scanning Image

zinc

steel

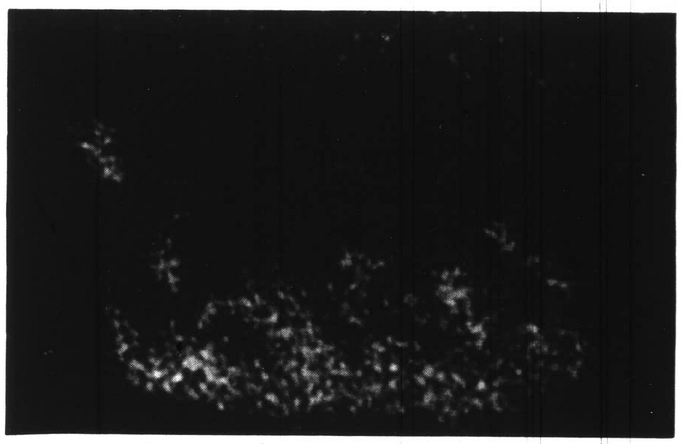

Aluminum Kα Radiation Image

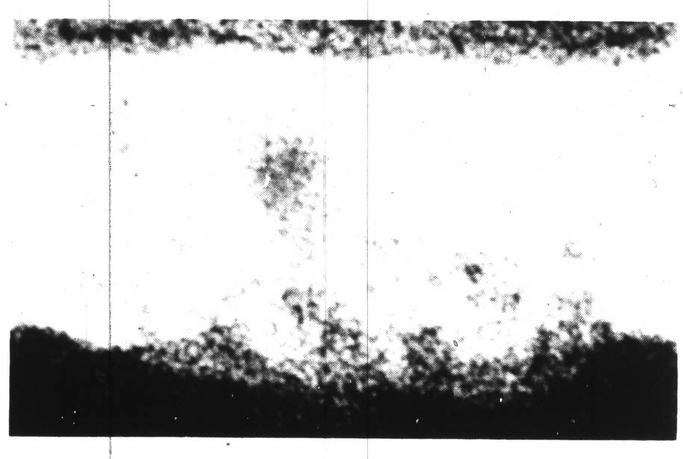

Zinc Kα Radiation Image

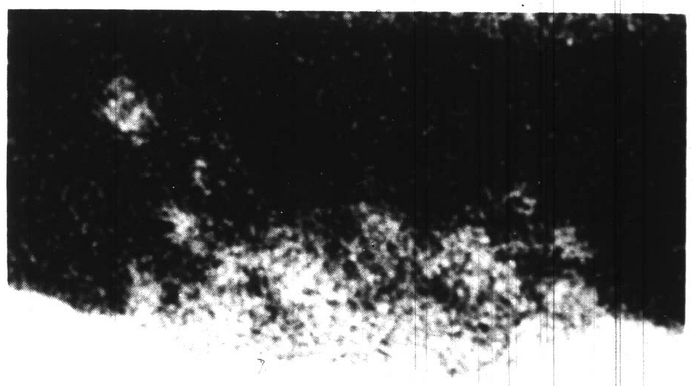

Iron Kα Radiation Image

FIGURE 19. Electron-Probe Microanalysis of Localized Growth on a 0.32 Per Cent Aluminum Coating with 0.004 Per Cent Iron which was made at 450°C with a 320 Second Immersion. 750X

Electron Scanning Image

copper

steel

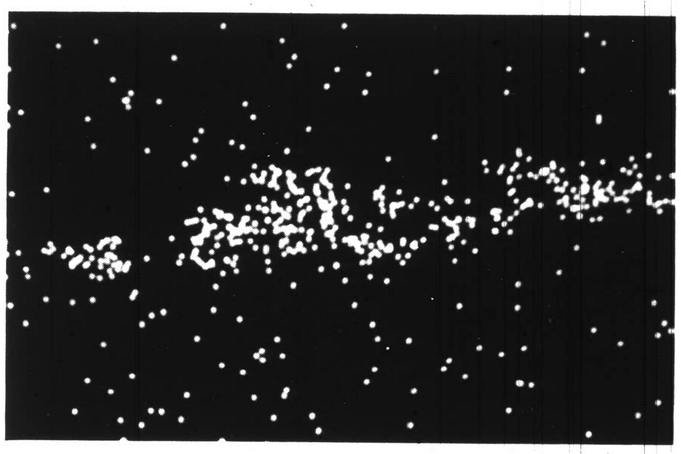

Aluminum Kα Radiation Image

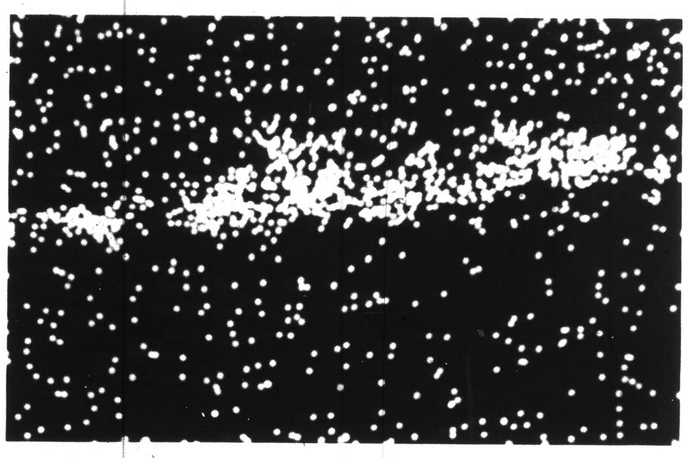

Zinc Kα Radiation Image

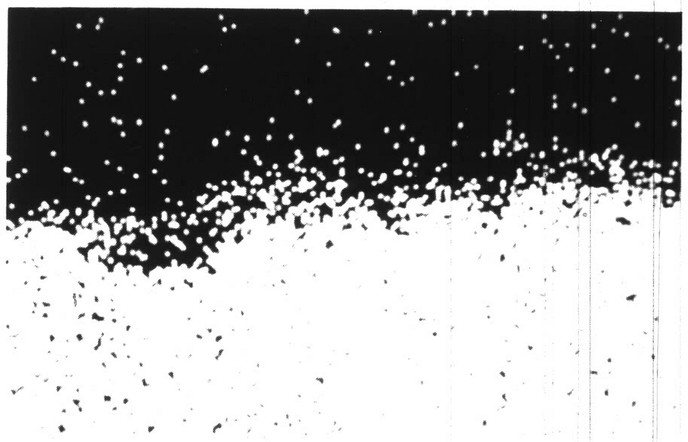

Iron Kα Radiation Image

FIGURE 20. Electron-Probe Microanalysis (Radiation Images) of Blue-Gray Phase on a 0.22 Per Cent Aluminum Coating with 0.014 Per Cent Iron which was made at 470°C with a 320 Second Immersion and which was Stripped of the Zinc Overlay and Subsequently Electroplated with Copper. 820X.

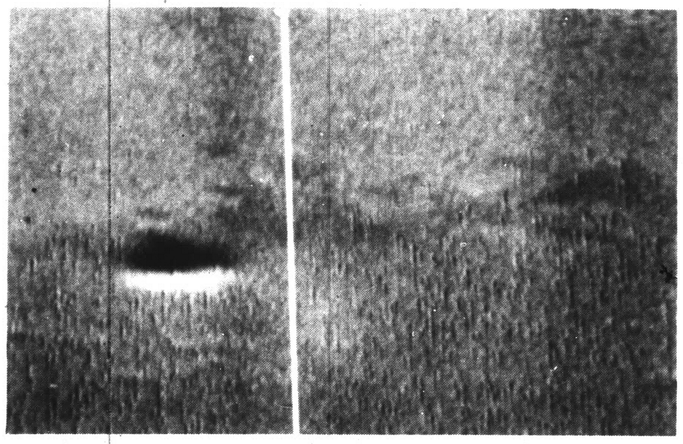

Electron Scanning Image

copper

steel

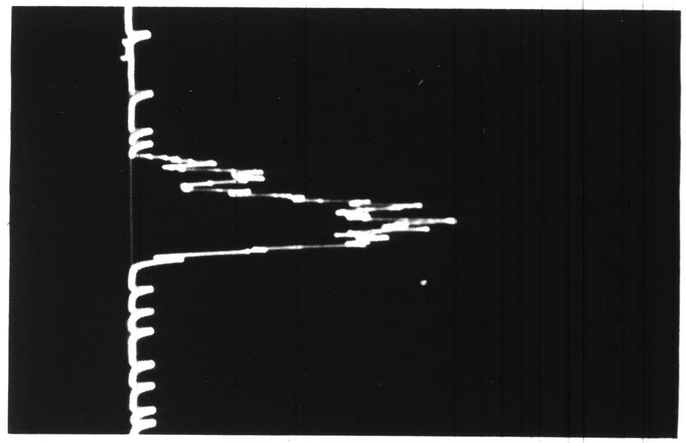

Aluminum Slow Scan 1000 cps

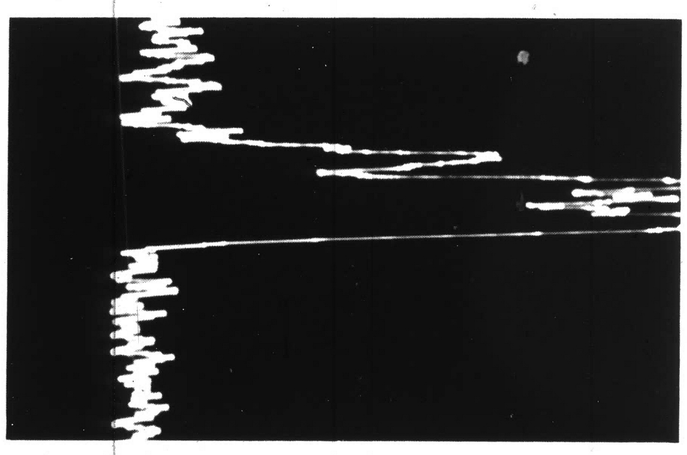

Zinc Slow Scan 1000 cps

Iron Slow Scan 30,000 cps

FIGURE 21. Electron-Probe Microanalysis (Line Scans) of Blue-Gray Phase on a 0.22 Per Cent Aluminum Coating with 0.014 Per Cent Iron which was made at 470°C with a 320 Second Immersion and which was Stripped of the Zinc Overlay and Subsequently Electroplated with Copper. 820X.

in Figure 7b. Both the radiation images and the line scans clearly show that iron, zinc and aluminum are present in the blue-gray phase particles.

Electron-probe point analyses of these same 0.22 and 0.32 per cent aluminum coatings are shown in Table 12. The microprobe analyses were obtained by comparing the intensities of iron, zinc, aluminum and copper with corresponding intensities from pure standards under the same excitation conditions. These data do not represent absolute values because they are not corrected for absorption or enhancement of X-rays but they are valid for comparison purposes. Again, iron, zinc and aluminum are present in the blue-gray phase particles as indicated in the radiation images and line scans. Notice, however, that the zinc background did give higher zinc intensities for the particles with the zinc overlay present than for those with an electroplated copper overlay. Although no specific composition is indicated by this microprobe analysis, these data clearly show that the blue-gray particle phase is a ternary iron-zinc-aluminum transition phase. This phase may be a non-equilibrium ternary compound or possibly an aluminum-rich iron-zinc compound or a zinc-rich iron-aluminum compound. Nevertheless, the existence of this ternary phase along with Fe_2Al_5 confirms the proposals made by Horstmann[23] and Cameron and Ormay[24].

TABLE 12

ELECTRON-PROBE POINT ANALYSIS OF BLUE-GRAY PHASE PARTICLES ON COATINGS CONTAINING ABOUT 0.20 AND 0.30 PER CENT ALUMINUM

Bath Composition	Coating Conditions	Analysis Al	Zn	Fe	Cu	Remarks
0.22% Al 0.012% Fe	430°C, 40 Sec. Immersion	6.0	45.6	24.9	--	Zinc overlay present
0.22% Al 0.014% Fe	470°C, 320 Sec. Immersion	8.0	38.0	28.1	--	Zinc overlay present
0.32% Al 0.004% Fe	450°C, 320 Sec. Immersion	10.5	21.4	35.6	--	Zinc overlay present
0.22% Al 0.014% Fe	470°C, 320 Sec. Immersion	4.1	8.0	24.0	33.7	Copper-electroplated

The definite identification that the blue-gray particle phase is a ternary phase now indicates that the growth curves obtained are an average of the individual growth rates of the thin-layered Fe_2Al_5 phase and the nodular or bursting ternary phase. Therefore, the total weight of alloy determined under any given condition will be a function of the amount of each phase present. Despite this dual growth of the aluminum-rich alloy layer, the combined growth of both phases was still parabolic for most conditions. The exception to this, however, was the coating which contained 0.22 per cent aluminum and 0.014 per cent iron and which was coated at 470°C with an immersion time of 320 seconds. Metallographic examination showed that this coating contained a large amount of the ternary phase. Thus, the weight of the ternary phase probably predominated for these conditions. As shown, this gave a much higher weight than similar composition coatings made at shorter times and, therefore, did not fit the parabolic growth curve shown in Figure 12.

Mechanism of Growth of the Aluminum-Rich Alloy Layer

This work confirms the findings previously reported by others that the formation of a layer of Fe_2Al_5 prevents the growth of iron-zinc alloy layers in zinc baths containing more than 0.20 per cent aluminum. However, the observations and data related to the formation of the ternary phase confirm the theory originally proposed by Horstmann[25] that breakdown of inhibition occurs by transformation of the Fe_2Al_5

layer to a ternary phase. The following hypothesis is suggested to explain these observations.

A layer of Fe_2Al_5 nucleates and grows on the surface of the steel during short immersions in the zinc bath at all temperatures. This initial stage of growth is characterized by the straight line interface shown in the metallographic examination and the smooth, compact surface layer shown in the electron microscope examination. No attack of the steel by the bath occurs at this time.

With longer immersion time, the zinc bath apparently reacts with the Fe_2Al_5 layer and nodules of the ternary phase begin to nucleate and grow on the surface as shown in the electron microscope examination. Thus, this suggests that as the nodules grow, the thin, protective layer of Fe_2Al_5 is probably being consumed. The initiating cause for nucleation of the ternary phase is not clear. However, it appears, as pointed out by Haughton[20], that the aluminum/iron ratio of the bath at these localized areas of nodule formation is important in favoring continued growth of the ternary phase. A comparison of the observations and data between the baths containing about 0.004 and about 0.013 per cent iron at about 0.20 per cent aluminum shows that nodule or ternary phase formation is favored by the higher iron content bath.

At even longer immersion times, nodules of the ternary phase continue to grow and coalesce, eventually forming loosely adherent layers which slough off into the bath. At this stage the Fe_2Al_5 layer

is consumed or penetrated, thereby exposing the steel base to the zinc bath and growth of iron-zinc phases can occur.

In general, this sequence of growth and breakdown of inhibition seems to be the same for all temperatures. However, at a given temperature, formation of the nodular ternary phase is favored by long immersion times, low aluminum and high iron contents in the bath. Conversely, formation of the protective Fe_2Al_5 layer is favored by short immersion time, high aluminum and low iron contents in the bath.

Practical Significance of this Work

Results from this work show that high aluminum/iron ratios should be maintained at the surface of the strip in continuous galvanizing baths for promotion of growth of the inhibiting Fe_2Al_5 layer. However, because continuous galvanizing baths are generally iron saturated, high aluminum/iron ratios must be achieved by maintaining proper aluminum levels with good bath agitation to make aluminum available to the strip surface. Conversely, these results show that subsequent processing of galvanized sheet to galvannealed sheet is enhanced by low aluminum/iron ratios which, in turn, promotes formation of the transition ternary phase and iron-zinc alloy layer growth.

This work has also provided a new method by which the formation and growth of the aluminum-rich alloy layer can be studied and related

to characteristics and properties of continuous galvanized coatings. Particularly, coating conditions, processing variables and bath composition can be studied for their effect on the aluminum-rich alloy layer. Moreover, the characteristics of the aluminum-rich alloy layers produced by the various continuous processes can also be studied. For example, continuous coatings produced by a gaseous surface preparation process may give a different characteristic aluminum-rich alloy layer than a flux process.

Results from such studies might then be applicable to properties of galvanized coatings which involve the aluminum-rich alloy layer such as coating ductility and adherence, weldability and corrosion resistance. Also, as mentioned, the aluminum-rich alloy layer must play a role in further processing of continuous galvanized coatings to galvannealed coatings. In fact, Bernick and Sievert[27] in work describing galvannealing conditions necessary to produce ductile galvannealed coatings recognized that aluminum in the zinc bath significantly affected the results.

Thus, such studies could lead to a better understanding of the continuous galvanizing process and the effect of the aluminum-rich alloy layer on the various properties of the galvanized coating.

CONCLUSIONS

The following conclusions have been drawn as a result of this work.

1. The formation of a protective aluminum-rich alloy layer on the surface of the steel inhibits iron-zinc alloy layer growth in aluminum-bearing zinc.
2. Growth of this aluminum-rich alloy layer occurs in stages. It is mainly comprised of Fe_2Al_5 in the early stages of growth. Later, transformation to an iron-zinc-aluminum ternary phase occurs locally and simultaneous growth of both Fe_2Al_5 and the ternary phase occurs.
3. The thickness of this aluminum-rich alloy layer in the early stages of growth for immersion times the order of those in continuous galvanizing is estimated to be about 0.1 micron (0.004 mil), or about equivalent to the thickness of the $FeSn_2$ layer on tinplate.
4. For most conditions, growth of this aluminum-rich alloy was parabolic for both early and intermediate stages of growth, even though Fe_2Al_5 and the ternary phase grow simultaneously.
5. Growth of the total aluminum-rich alloy layer is controlled by the bath temperature and the aluminum and iron contents of the zinc bath. At temperatures of 450°C and 470°C,

the aluminum/iron ratio of the bath has a particularly strong effect on the growth of this layer; low ratios favor faster growth rates and high ratios favor slower growth rates.

6. These same conditions of high temperature, long immersion times and lower aluminum/iron bath ratios also seem to favor transformation to the ternary phase. Conversely, lower temperatures, shorter immersion times and higher aluminum/iron bath ratios favor growth of Fe_2Al_5.

7. Breakdown of inhibition occurs when the Fe_2Al_5 layer is consumed or penetrated during the transformation to the ternary phase. At this advanced stage, loosely adherent particles of ternary phase slough off into the bath, exposing the steel base to the bath and allowing growth of iron-zinc phases to occur.

APPENDIX

Method Used to Electroplate Copper on the Aluminum-Rich Alloy Layer on Coatings Stripped of The Zinc Overlay in the Sulfuric Acid-Arsenite Solution.

The following method was reported to the writer by S. E. Rauch of Homer Research Laboratories, Bethlehem Steel Corporation, who used this technique during metallographic studies of the $FeSn_2$ alloy layer on tinplate.

A cyanide plating bath was used which was prepared by diluting the following reagents in water to 1500 milliliters:

180 grams cuprous cyanide

246 grams sodium cyanide

45 grams sodium hydroxide

A copper sheet was used as an anode and copper was electroplated on the stripped overlay specimen cathode at a current density of about 6 amps per square foot at about 4 volts. Current was applied for about two hours which gave copper coating thicknesses of about 2 to 3 mils.

A 12 volt battery eliminator was used for the power supply with variable resistors in the circuit to adjust the current to about 0.2 amp. Specimens used were about 2 inches x 2.25 inches.

REFERENCES

1. Bablik, H., Galvanizing (Hot Dip), 3rd Edition, Spon. Ltd., London, England (1950), p. 204.

2. Thorley, R. W., "Factors Affecting the Production and Properties of Hot Dipped Galvanized Coatings: A Review of Literature", British Non-Ferrous Metals Research Association, Research Report No. A868, January, 1950.

3. Hughes, M. L., "Use of Aluminum in Hot-Dip Galvanizing", Journal of the Iron and Steel Institute, September, 1950, pp. 77-84.

4. Hughes, M. L., "The Influence of Aluminum on the Alloying Action in Hot Dip Galvanizing", Proceedings of the International Conference on Hot Dip Galvanizing Held at Copenhagen 17-21 July 1950, Zinc Development Association, Oxford, England, (March 1951) pp. 31-43.

5. Haughton, M. A., "The Effect of Aluminum and Iron on the Structure of Galvanized Coatings", Proceedings of the Second International Conference on Hot Dip Galvanizing Held at Dusseldorf 30th June - 4th July 1952, Zinc Development Association, Oxford, England, (July 1953) pp. 59-87.

6. Bablik, H., Gotzl, F. and Kukaczka, R., "The Causes of the Retarding Effect of Aluminum in Galvanizing Baths", Werkstoffe u. Korrosion, Vol. 2, 1951, pp. 1963-1965.

7. Horstmann, D., "The Inhibiting Effect of Aluminum in Hot Galvanizing Baths on the Formation of the Iron-Zinc-Alloy Layers", Arch. Eisenhutt., May 1956, pp. 297-302.

8. Sebisty, J. J. and Edwards, J. O., "The Influence of Aluminum, Lead and Iron on the Structure and Properties of Galvanized Coatings", Proceedings of the Fifth International Conference on Hot Dip Galvanizing, Zinc Development Association, London, England, (1959), pp. 213-240.

9. Cameron, D. I. and Ormay, M. K., "The Effects of Agitation, Cooling and Aluminum on the Alloying in Hot Dipping in Zinc", Proceedings of the 6th International Conference on Hot Dip Galvanizing, Interlaken, June 1961, Zinc Development Association, London, England (1962), pp. 276-316.

10. Ibid., p. 304

11. Guertler, W., Guertler, M. and Anastasiadias, E., A Compendium of Constitutional Ternary Diagrams of the Metallic Systems, WADC-TR-58-615, Part III, Directorate of Materials and Processes, Wright-Patterson Air Force Base, Ohio, (March, 1962), pp. 210-213.

12. Raynor, G. V., Faulkner, C. R., Noden, J. D., and Harding, A. R., "Ternary Alloys Formed by Aluminum, Transitional Metals and Divalent Metals, Acta Metallurgica, Vol. 1, November 1953, pp. 629-647.

13. Gebhardt, E., "Investigations into the Ternary System Aluminum-Iron-Zinc", Zeitschrift fur Metallkunde, Vol. 44, No. 5, 1953, pp. 206-211. (Brutcher Translation No. 3269).

14. Rennhack, E. H., "Zinc-Rich Corner of the Zn-Fe-Al System", Transactions of the Metallurgical Society of AIME, Vol. 221, August 1961, pp. 775-779.

15. Southin, R. T. and Wright, D. A., "Fe_2Al_5 and FeSi in Zinc Alloys", Journal of the Institute of Metals, 1965, pp. 357-358.

16. Haughton, loc. cit.

17. Ikenberry, L. C., "Determining the Weight and Analyses of Unalloyed and Alloyed Coating Layers on Hot-Dipped Aluminum-Coated Steel", Materials Research and Standards, March 1962, pp. 177-179.

18. Haughton, loc. cit.

19. Davies, J. E. and Hoare, W. E., "Metallography of Electro-Tinplate", Journal of the Iron and Steel Institute, June 1951, pp. 134-140.

20. Kunze, C. T. and Willey, A. R., "Electrolytic Determination of Tin and Tin-Iron Alloy Coating Weights on Tin Plate", Journal of the Electrochemical Society, Vol. 99, No. 9, September 1952, pp. 354-359.

21. Ikenberry, loc cit.

22. Frame, J. W., "A Study of the Mechanism Controlling the Presence and Relative Thickness of Alloy Layers in Iron-Aluminum Diffusion Couples", Unpublished Thesis, Lehigh University, May 1961.

23. Horstmann, loc. cit.

24. Cameron and Ormay, loc. cit.

25. Horstmann, loc. cit.

26. Haughton, loc. cit.

27. Bernick, L. M. and Sievert, W. C., "Processing of Galvannealed Sheet", Presented at the First Operating Metallurgy Conference of A.I.M.E., December 2, 1965.

VITA

Angelo Richard Borzillo, son of the late Anthony M. and Sarah (Marino) Borzillo, was born in Norristown, Pennsylvania on May 19, 1933. He attended the elementary schools of Bridgeport, Pennsylvania and graduated from Bridgeport High School in May 1951. In June 1955, he graduated from the Pennsylvania State University with a Bachelor of Science Degree in Metallurgy and was commissioned a Second Lieutenant in the United States Army Corps of Engineers.

Mr. Borzillo was employed as a Looper Trainee by the Bethlehem Steel Corporation in July of 1955 and was later assigned to the Corrosion Group of the Research Department. In March 1956 he entered the United States Army for a six-month tour of active duty and then served in the Ready and Standby Reserves until June of 1963.

In the Corrosion Group of the Research Department, Mr. Borzillo was involved mainly in studies of the corrosion of steel products in natural media and in development of hot dip alloy coatings. In June of 1967, he was reassigned to the Sheet and Tin Mill Products Section, where he is now following the processing and testing of pilot line produced chromized steel.

Mr. Borzillo enrolled in Lehigh University as a part-time industrial graduate student in September of 1962. He is a member of the National Association of Corrosion Engineers and ASTM Committees A-5, Metallic Coated Iron and Steel Products, and G-1, Corrosion of Metals.

Mr. Borzillo is married to the former Lucia Cantello of Norristown, Pennsylvania, and is the father of two sons, Anthony and Robert, whose present ages are 9 and 7, respectively.